



Static polarizabilities for excited states within the spin-conserving and spin-flipping equation-of-motion coupled-cluster singles and doubles formalism: Theory, implementation, and benchmarks

Kaushik D. Nanda and Anna I. Krylov

Citation: *The Journal of Chemical Physics* **145**, 204116 (2016); doi: 10.1063/1.4967860

View online: <http://dx.doi.org/10.1063/1.4967860>

View Table of Contents: <http://scitation.aip.org/content/aip/journal/jcp/145/20?ver=pdfcov>

Published by the AIP Publishing

Articles you may be interested in

Double spin-flip approach within equation-of-motion coupled cluster and configuration interaction formalisms: Theory, implementation, and examples

J. Chem. Phys. **130**, 044103 (2009); 10.1063/1.3066652

Dyson orbitals for ionization from the ground and electronically excited states within equation-of-motion coupled-cluster formalism: Theory, implementation, and examples

J. Chem. Phys. **127**, 234106 (2007); 10.1063/1.2805393

Spin-conserving and spin-flipping equation-of-motion coupled-cluster method with triple excitations

J. Chem. Phys. **123**, 084107 (2005); 10.1063/1.2006091

Analytic gradients for the spin-conserving and spin-flipping equation-of-motion coupled-cluster models with single and double substitutions

J. Chem. Phys. **122**, 224106 (2005); 10.1063/1.1877072

Equation-of-motion spin-flip coupled-cluster model with single and double substitutions: Theory and application to cyclobutadiene

J. Chem. Phys. **120**, 175 (2004); 10.1063/1.1630018

An advertisement for AIP Applied Physics Reviews. It features a circular inset showing a microscopic image of a lithium niobate crystal with various layers and labels. To the right of the inset, the text "NEW Special Topic Sections" is displayed in large, bold, white letters against a blue background. Below this, the text "NOW ONLINE" is in yellow, followed by "Lithium Niobate Properties and Applications: Reviews of Emerging Trends". At the bottom right, the AIP logo is shown with the text "AIP | Applied Physics Reviews".

AIP Applied Physics Reviews

NEW Special Topic Sections

NOW ONLINE

Lithium Niobate Properties and Applications:
Reviews of Emerging Trends

AIP | Applied Physics Reviews

Static polarizabilities for excited states within the spin-conserving and spin-flipping equation-of-motion coupled-cluster singles and doubles formalism: Theory, implementation, and benchmarks

Kaushik D. Nanda and Anna I. Krylov

Department of Chemistry, University of Southern California, Los Angeles, California 90089-0482, USA

(Received 25 August 2016; accepted 2 November 2016; published online 30 November 2016)

We present the theory and implementation for calculating static polarizabilities within the equation-of-motion coupled-cluster singles and doubles (EOM-CCSD) framework for electronically excited states and its spin-flip variant. We evaluate the second derivatives of the EOM-CCSD Lagrangian with respect to electric-field perturbations. The relaxation of reference molecular orbitals is not included. In our approach, the wave function amplitudes satisfy the $2n + 1$ rule and the amplitude-response Lagrange multipliers satisfy the $2n + 2$ rule. The new implementation is validated against finite-field and CCSD response-theory calculations of the excited-state polarizabilities of pyrimidine and s-tetrazine. We use the new method to compute static polarizabilities of different types of electronic states (valence, charge-transfer, singlets, and triplets) in open- and closed-shell systems (uracil, *p*-nitroaniline, methylene, and *p*-benzyne). We also present an alternative approach for calculating excited-state static polarizabilities as expectation values by using the EOM-CCSD wave functions and energies in the polarizability expression for an exact state. We find that this computationally less demanding approach may show differences up to $\sim 30\%$ relative to the excited-state polarizabilities computed using the analytic-derivative formalism. Published by AIP Publishing. [<http://dx.doi.org/10.1063/1.4967860>]

I. INTRODUCTION

Dipole polarizability (α) describes the second-order response of system's energy and the linear response of its dipole moment (μ) in the presence of electric-field perturbations (ϵ). The definition is based on the Taylor expansion of the energy in the presence of external electric-field perturbations:

$$E = E_0 - \sum_I \mu_I \epsilon_I - \sum_{IJ} \frac{1}{2} \alpha_{IJ} \epsilon_I \epsilon_J - \dots, \quad (1)$$

where ϵ_I and ϵ_J are the Cartesian components of the perturbations. In the static limit, the components of the dipole polarizability are given by the second derivative of the energy (or the first derivative of the dipole moment) with respect to these electric-field perturbations. The dipole polarizability of an exact state Ψ_k with energy E_k is given by the following expression:^{1,2}

$$\alpha_{xy}^k(\omega, -\omega) = \sum_{n \neq k} \left(\frac{\langle \Psi_k | \mu_x | \Psi_n \rangle \langle \Psi_n | \mu_y | \Psi_k \rangle}{E_n - E_k - \omega} + \frac{\langle \Psi_k | \mu_y | \Psi_n \rangle \langle \Psi_n | \mu_x | \Psi_k \rangle}{E_n - E_k + \omega} \right), \quad (2)$$

where μ_x is the dipole moment operator of the system interacting with the electric-field perturbation with frequency ω in the x -direction and the sum-over-states runs over the ground and all excited states except Ψ_k . The poles of the polarizability yield the electronic spectrum of the system. The sum-over-states expression suggests large static polarizabilities for states that are coupled to closely lying electronic states by large transition dipole moments.

Macroscopically, the polarizability of a substance is related to its refractive index (via the Lorentz-Lorenz equation) and dielectric constant (via the Clausius-Mossotti equation). The polarizability of a molecule is an important quantity for understanding its interactions with the environment.^{3,4} The ground- and excited-state polarizabilities are related to the intermolecular dispersion interactions. For example, the van der Waals dispersion coefficient for the R^{-6} -term, which describes the attractive interactions between non-polar species, depends on their polarizabilities.⁴⁻⁶ Gas-phase excited-state polarizabilities of non-polar molecules can be measured directly with laser Stark spectroscopy;^{7,8} however, theory is often needed for estimating and assigning individual polarizability tensor components.

The focus of many previous theoretical studies has been on the accurate calculations of ground-state polarizabilities,^{5,9-12} few calculations for the excited-state polarizabilities have been reported.^{4,13-21} In some studies, calculations of the excited-state static polarizabilities have been performed using the finite-field approach, i.e., by numerical differentiation of the excited-state energies or dipole moments under perturbing external electric fields. To list a few examples, finite-field excited-state polarizabilities have been reported by Sadlej, Urban, and co-workers using complete active space self-consistent field (CASSCF)¹³ and perturbation theory corrected CASSCF (CASPT2)⁴ energies, by Medved *et al.* using time-dependent density functional theory (TDDFT) energies,¹⁴ and by Stanton and Gauss using equation-of-motion coupled-cluster with single and double substitutions (EOM-CCSD) dipole moments.¹⁵ Despite their conceptual simplicity, there are several concerns associated with the finite-field

approaches. First, finite-field calculations may suffer from numerical precision problems. Second, these finite-field differences cannot be used for calculating frequency-dependent (dynamic) polarizabilities. Third, symmetry is reduced (or lost) in finite-difference calculations, which increases the cost of the calculations. Fourth, one can encounter numeric problems with closely lying electronic states changing their relative order at different field values. Therefore, efficient analytical methods for describing excited-state static and dynamic polarizabilities are desirable.

Both static and frequency-dependent polarizabilities can be evaluated using the response-theory approach, wherein the response to a time-periodic perturbation is described by its exponentially parameterized time evolution. Within response theory, excited-state polarizabilities can be formulated in two different ways. In the first approach, excited-state polarizability is obtained as linear response function of the excited-state wave function. In the second approach, the difference between the polarizabilities of an excited state and the ground state is calculated as the double residue of the cubic response function of the ground-state wave function. Implementations for excited-state polarizabilities using the latter strategy have been reported for SCF¹⁶ and CASSCF^{17,18} wave functions and TDDFT.¹⁹ The double-residue approach, however, leads to numerical problems due to secular divergences in the static limit. Hättig *et al.* have reported an implementation for various coupled-cluster methods including CCS (coupled-cluster singles), CC2 (a second-order approximation to CCSD) and CCSD, wherein the excited-state polarizabilities are obtained as the analytic-second derivatives of the excited-state quasienergy Lagrangian while avoiding these divergences.²⁰ Using this strategy, Graf *et al.* have recently implemented excited-state polarizabilities for the CC2 method with the resolution-of-the-identity approximation.²¹

Gauss and co-workers have discussed the similarities between analytic derivatives of the energy and the response-theory approach for coupled-cluster methods.¹² For coupled-cluster ground states, they have demonstrated that the code for static polarizabilities as second derivatives can be extended by small modifications to the calculations of frequency-dependent polarizabilities. Thus, as an alternative to the response-theory approach, one can use the analytic-derivative approach as the starting point in a general formalism for calculating the static and frequency-dependent polarizabilities of the coupled-cluster ground state. Here, we follow this strategy and present the implementation for calculating the excited-state static polarizabilities as analytic second derivatives of the excited-state energy within the EOM-CCSD framework for electronically excited (EOM-EE-CCSD) and spin-flipped (EOM-SF-CCSD) target states. Our approach for excited-state static polarizabilities can be extended to calculate frequency-dependent polarizabilities.

The EOM-CC methods provide a robust and accurate description of excited states in a variety of closed- and open-shell species within a single-reference framework.^{22–28} The EOM-CC methods, which enable accurate calculations of energy differences between different electronic states (excitation, ionization, and electron-attachment energies), also provide a convenient framework for calculating various

properties²⁹ such as solvatochromic shifts,³⁰ dipole moments, transition dipole moments, two-photon absorption cross-sections,³¹ and spin-orbit couplings^{32,33} for closed- and open-shell species.³⁴ Finite-field calculations for the ground- and excited-state polarizabilities of s-tetrazine using the EOM-EE-CCSD dipole moments have also been reported by Stanton and Gauss.¹⁵ The same authors also presented the derivations of the analytic first and second derivatives^{35,36} of the EOM-EE-CCSD energies. Although implementations of the analytic gradients for the EOM-CC methods have been reported by several groups,^{37,38} this work and Ref. 39 are the first implementations for polarizabilities of the EOM-(EE/SF)-CCSD and EOM-IP-CCSD (EOM-CCSD for ionized states) states using the analytic-derivative approach. In Ref. 36, the second derivatives of the EOM-EE-CC energy have been formulated using two different derivations leading to the final expression, which is either symmetric or asymmetric with respect to the interchange of the two external electric-field perturbations. While the perturbed parameters with respect to only one of the two perturbations are required in the asymmetric formulation, more response equations are solved relative to the symmetric formulation. In this work, we report and discuss the analytic implementation of the excited-state static polarizabilities based on a mixed symmetric-asymmetric formulation of the second derivatives of the EOM-(EE/SF)-CCSD energies.

Following the strategy used in the derivation of the excited-state energy gradients,^{38,40–44} we employ the EOM-CCSD Lagrangian for the excited-state energy. Our implementation for calculating the excited-state static polarizabilities satisfies Wigner's $2n + 1$ rule^{45,46} for the wave function parameters (CCSD T -amplitudes, EOM-CCSD R - and L -amplitudes) and a stronger $2n + 2$ rule for the amplitude-response Lagrange multipliers formulated by Helgaker and Jørgensen^{47,48} (note that EOM-CCSD L -amplitudes can also be viewed as Lagrange multipliers). Similarly to the coupled-cluster response theory, we do not include the relaxation of the reference molecular orbitals in the presence of the electric-field perturbations; only the cluster amplitudes and the EOM-CCSD wave function amplitudes are allowed to relax. The relaxation of the reference determinant is usually excluded because it introduces unphysical poles in the response functions.^{2,49} Our implementation is similar to the unrelaxed analytic derivatives for the static ground-state properties developed by Gauss and co-workers.¹² We explicitly avoid secular divergences by solving the response equations for the first-order EOM-CCSD amplitudes in the biorthogonal space of the excited-state's left- and right-eigenfunctions. For non-degenerate target states, this approach results in stable numerical behavior in the static limit.

We also explore an alternative approach in which the polarizabilities are computed as expectation values by using EOM-CCSD wave functions and energies in the polarizability expression for an exact state given by Eq. (2). Bartlett and co-workers have shown that this approach yields CCSD ground-state polarizabilities⁵ and first hyperpolarizabilities⁵⁰ that differ only slightly from the response-theory results despite the (small) violation of size-extensivity. Recently, we have exploited this approach in the

EOM-EE-CCSD implementation for calculating two-photon absorption cross-sections; we found that these cross-sections are similar in quality to the CCSD response-theory results.³¹ A recently reported EOM-CCSD implementation for calculating spin-orbit couplings also employs the expectation-value approach.³³ The expectation-value approach for calculating the higher-order properties is significantly less demanding in terms of computational costs. Here, we compare the formalisms, the computational costs, and the accuracy of the analytic-derivative and the expectation-value approaches for calculating the ground- and excited-state static polarizabilities. We also note that the response properties obtained with the expectation-value approach are equivalent to those obtained with the so-called coupled cluster-configuration interaction (CC-CI) response-theory approach, wherein the time-evolution of the unperturbed coupled-cluster state is linearly parameterized, in contrast to the exponential parameterization in the regular coupled-cluster response theory.^{51,52}

We use our implementation to study the relationship between the underlying electronic structure and polarizabilities by considering singlet and triplet valence $\pi \rightarrow \pi^*$ and $n \rightarrow \pi^*$ states in closed-shell systems (pyrimidine, s-tetrazine, uracil) as well as charge-transfer states (in *para*-nitroaniline). Recently, there has been a surge of interest in open-shell systems as building blocks for materials with tunable non-linear properties such as polarizabilities, two-photon absorption cross sections, and hyperpolarizabilities.^{53–57} Our EOM-CCSD implementation enables calculations of static polarizabilities of open-shell species for which such predictions are scarce. Further, these implementations allow us to investigate fundamental questions pertaining to the effects of electronic structure and open-shell character on polarizabilities, which is important in the rational design of non-linear materials. Here, we consider two prototypical diradicals: methylene and *para*-benzyne.

The structure of the paper is as follows. In Section II A, we revisit the EOM-EE-CCSD and EOM-SF-CCSD theories. In Sections II B and II C, we outline the formalism of the CCSD energy Lagrangian and its first and second derivatives with respect to electric-field perturbations and discuss our implementation of the CCSD static polarizabilities. In Sections II D and II E, we present the derivation of the EOM-CCSD static polarizabilities as second derivatives of the EOM-CCSD energy Lagrangian. In Section II F, we discuss the formalism and implementation for calculating polarizabilities with the expectation-value approach. Sections III and IV present the computational details and results for excited-state polarizabilities for our benchmark systems (pyrimidine and s-tetrazine) as well as other closed-shell systems such as uracil and *p*-nitroaniline, and open-shell diradicals (methylene and *p*-benzyne).

II. THEORY

A. Equation-of-motion coupled-cluster method with single and double substitutions

The EOM-CC approach provides an efficient strategy for describing multiple electronically excited states of closed- and

open-shell species, including those with multi-configurational wave functions, in a single-reference framework. In contrast to the state-specific multireference methods, the EOM methods describe the entire manifold of target states by employing a linear parameterization of excitation operators in the Fock space acting on a single-reference state. The EOM-CCSD wave function is given by the following ansatz:

$$|\Psi\rangle = Re^T |\Phi_0\rangle, \quad (3)$$

where the linear EOM operator R acts on the reference CCSD wave function, $e^T |\Phi_0\rangle$. The cluster operator T and EOM operator R are excitation operators given as sum of single and double excitation operators:

$$T = T_1 + T_2 \quad \&& \quad R = r_0 + R_1 + R_2, \quad (4)$$

where r_0 is defined below (Eq. (20)) and

$$T_1 = \sum_{ia} t_i^a a^+ i; \quad T_2 = \frac{1}{4} \sum_{ijab} t_{ij}^{ab} a^+ b^+ ji; \quad (5)$$

$$R_1 = \sum_{ia} r_i^a a^+ i; \quad R_2 = \frac{1}{4} \sum_{ijab} r_{ij}^{ab} a^+ b^+ ji \quad (6)$$

for the EE and SF variants of EOM-CCSD. T satisfies the reference-state CCSD equations,

$$\langle \Phi_\mu | \bar{H} | \Phi_0 \rangle = 0, \quad (7)$$

where Φ_μ are the μ -tuple ($\mu = 1, 2$) excited (with respect to the reference determinant,⁵⁸ Φ_0) determinants and $\bar{H} = e^{-T} H e^T$ is the similarity-transformed Hamiltonian. The reference CCSD energy is given by

$$\langle \Phi_0 | \bar{H} | \Phi_0 \rangle = E_{CCSD} = E_0. \quad (8)$$

The EOM energies and amplitudes (r_i^a and r_{ij}^{ab}) are found by diagonalizing \bar{H} in the space of target configurations defined by the choice of operator R and reference determinant Φ_0 . In other words, different target states are accessed by different choices of the EOM operator and Ref. 25. In EOM-EE-CCSD, the EOM operators are electron- and spin-conserving and the reference corresponds to the ground-state wave function. In EOM-SF-CCSD, the EOM operators are electron-conserving but not spin-conserving and act on a high-spin reference to yield low-spin target states. EOM-SF provides a balanced treatment of multiconfigurational target states arising due to orbital degeneracies in diradicals, triradicals, and in bond-breaking reactions. The EOM-EE-CCSD and EOM-SF-CCSD equations in the spin-orbital basis are identical (only the spin-symmetry of the EOM amplitudes is different).

Because \bar{H} is non-Hermitian, its k th left and right eigenstates, $(L^k)^\dagger$ and R^k , are not Hermitian conjugates but form a biorthogonal set,

$$\bar{H} R^k = E_k R^k, \quad (9)$$

$$(L^k)^\dagger \bar{H} = (L^k)^\dagger E_k, \quad (10)$$

$$\langle \Phi_0 | L^m | R^n | \Phi_0 \rangle = \delta_{mn}, \quad (11)$$

where $L = L_1 + L_2 = \sum_{ia} l_i^a a^+ i + \frac{1}{4} \sum_{ijab} l_{ij}^{ab} a^+ b^+ j i$. For energy calculations, only right eigenstates are needed; however, both left and right eigenstates are needed for properties.

In the basis of the reference, singly, and doubly excited determinants, \bar{H} has the following form:

$$\bar{H} = \begin{pmatrix} E_0 & \bar{H}_{01} & \bar{H}_{02} \\ 0 & \bar{H}_{11} & \bar{H}_{12} \\ 0 & \bar{H}_{21} & \bar{H}_{22} \end{pmatrix}, \quad (12)$$

where the zero-blocks are due to the CCSD Eq. (7). The right and left EOM-CCSD eigenvalue equations are

$$(\bar{H} - E_0)R^k = (E_k - E_0)R^k = \Omega_k R^k, \quad (13)$$

$$L^k(\bar{H} - E_0) = L^k(E_k - E_0) = L^k\Omega_k, \quad (14)$$

$$\Omega_k = E_k - E_0. \quad (15)$$

In the matrix form,

$$\begin{pmatrix} \bar{H}_{11} - E_0 & \bar{H}_{12} \\ \bar{H}_{21} & \bar{H}_{22} - E_0 \end{pmatrix} \begin{pmatrix} R_1^k \\ R_2^k \end{pmatrix} = \Omega_k \begin{pmatrix} R_1^k \\ R_2^k \end{pmatrix}, \quad (16)$$

$$\begin{pmatrix} L_1^k & L_2^k \end{pmatrix} \begin{pmatrix} \bar{H}_{11} - E_0 & \bar{H}_{12} \\ \bar{H}_{21} & \bar{H}_{22} - E_0 \end{pmatrix} = \begin{pmatrix} L_1^k & L_2^k \end{pmatrix} \Omega_k. \quad (17)$$

Eqs. (13) and (14) are solved iteratively using Davidson procedure, which involves calculations of the σ - and $\tilde{\sigma}$ -vectors:

$$\begin{pmatrix} (\bar{H}_{11} - E_0)R_1^k + \bar{H}_{12}R_2^k \\ \bar{H}_{21}R_1^k + (\bar{H}_{22} - E_0)R_2^k \end{pmatrix} = \begin{pmatrix} \sigma_1^k \\ \sigma_2^k \end{pmatrix}, \quad (18)$$

$$\begin{pmatrix} L_1^k(\bar{H}_{11} - E_0) + L_2^k\bar{H}_{21} & L_1^k\bar{H}_{12} + L_2^k(\bar{H}_{22} - E_0) \end{pmatrix} = \begin{pmatrix} \tilde{\sigma}_1 & \tilde{\sigma}_2^k \end{pmatrix}. \quad (19)$$

The programmable expressions for the σ - and $\tilde{\sigma}$ -vectors are given in Ref. 59. The weight of the reference determinant in the right EOM-CCSD eigenvector, r_0 , is defined according to the following equation:

$$r_0^k = \frac{1}{\Omega_k} (\bar{H}_{01}R_1^k + \bar{H}_{02}R_2^k). \quad (20)$$

In the EOM-SF states, $r_0 = 0$ because the reference and the EOM determinants have a different number of α and β electrons.

B. CCSD Lagrangian and dipole moment

The CCSD Lagrangian depends on the T - and Λ -amplitudes:

$$\begin{aligned} \mathcal{L}(T, \Lambda) &= \langle \Phi_0 | e^{-T} H e^T | \Phi_0 \rangle + \sum_{\mu=1}^2 \lambda_\mu \langle \Phi_\mu | e^{-T} H e^T | \Phi_0 \rangle \\ &= \langle \Phi_0 | e^{-T} H e^T | \Phi_0 \rangle + \langle \Phi_0 \Lambda | e^{-T} H e^T | \Phi_0 \rangle, \end{aligned} \quad (21)$$

where the first term is the CC energy, the second term represents the constraints imposed by the coupled-cluster equations (Eq. (7)), and Λ are the Lagrange multipliers. This Lagrangian can be made stationary with respect to all parameters, meaning $\frac{\partial \mathcal{L}}{\partial T} = 0$ and $\frac{\partial \mathcal{L}}{\partial \Lambda} = 0$. Then, the first derivative of the CCSD

energy (which equals the first derivative of the Lagrangian) is given by the partial derivative of the Lagrangian:

$$\begin{aligned} \frac{dE_0}{d\epsilon} &= \frac{d\mathcal{L}}{d\epsilon} = \frac{\partial \mathcal{L}}{\partial \epsilon} + \frac{\partial \mathcal{L}}{\partial T} \frac{\partial T}{\partial \epsilon} + \frac{\partial \mathcal{L}}{\partial \Lambda} \frac{\partial \Lambda}{\partial \epsilon} = \frac{\partial \mathcal{L}}{\partial \epsilon} \\ &= \langle \Phi_0 (1 + \Lambda) | e^{-T} \frac{\partial H}{\partial \epsilon} e^T | \Phi_0 \rangle, \end{aligned} \quad (22)$$

where $\frac{\partial H}{\partial \epsilon}$ contains the explicit dependence of the Hamiltonian on the perturbation.

The reference Slater determinant, Φ_0 , is an anti-symmetrized direct product of molecular orbitals (MOs):

$$\Phi_0 = \mathcal{P}_{ij\dots}^-(\phi_i \otimes \phi_j \otimes \dots), \quad \phi_p = \sum_\mu C_{\mu p} \chi_\mu, \quad (23)$$

where ϕ s are the MOs and χ s are the atomic basis functions. The terms involving $\frac{\partial \Phi_0}{\partial \epsilon}$ in the above partial derivative of the CCSD Lagrangian are set to zero, because we exclude the parametric dependence of the MO coefficient matrix, C , on the electric-field perturbations ($\frac{\partial C}{\partial \epsilon} = 0$) and the basis functions do not depend on the electric field ($\frac{\partial \chi}{\partial \epsilon} = 0$).

In the presence of an electric-field perturbation, the perturbed Hamiltonian has only first-order terms in the perturbation and is given by

$$H = H^{(0)} - \vec{\epsilon} \cdot \vec{\mu} = H^{(0)} - \epsilon_x \mu_x e^{-i\omega_x t}, \quad (24)$$

where we assume, for simplicity, that the perturbing electric field is polarized along one of the Cartesian axes (here, x). In the static limit,

$$\lim_{\omega \rightarrow 0} \frac{\partial H}{\partial \epsilon_x} = -\mu_x. \quad (25)$$

The negative of the first derivative of the CCSD energy with respect to the electric-field perturbation equals the dipole moment of the CCSD state and is given by

$$\mu_x^0 = \langle \Phi_0 (1 + \Lambda) | e^{-T} \mu_x e^T | \Phi_0 \rangle. \quad (26)$$

The dipole moment can be computed using the one-particle density matrix as

$$\mu_x^0 = \sum_{pq} \gamma_{pq} \mu_{x,pq}, \quad (27)$$

where γ_{pq} is

$$\gamma_{pq} \equiv \langle \Phi_0 (1 + \Lambda) | e^{-T} | p^+ q | e^T \Phi_0 \rangle. \quad (28)$$

The programmable expressions for the different (occupied-occupied, occupied-virtual, virtual-occupied, and virtual-virtual) blocks of the CCSD density matrix are given in the supplementary material.

C. CCSD static polarizabilities as analytic derivatives

In the presence of two electric-field perturbations, the perturbed electronic Hamiltonian is given by

$$H = H^{(0)} - \epsilon_x \mu_x e^{-i\omega_x t} - \epsilon_y \mu_y e^{-i\omega_y t} \quad (29)$$

so that in the static limit

$$\lim_{\omega_x \rightarrow 0} \frac{\partial H}{\partial \epsilon_x} = -\mu_x \quad \& \quad \lim_{\omega_y \rightarrow 0} \frac{\partial H}{\partial \epsilon_y} = -\mu_y. \quad (30)$$

The CCSD static polarizability is the negative of the second derivatives of the CCSD energy with respect to two electric-field perturbations or, equivalently, the first derivative of the

dipole moment with respect to the electric-field perturbation (polarizability is positive when the magnitude of the dipole moment increases due to a parallel electric field):

$$\begin{aligned}\alpha_{xy}^0 &= \frac{d\mu_x^0}{d\epsilon_y} \\ &= \langle \Phi_0 \frac{\partial \Lambda}{\partial \epsilon_y} | \bar{\mu}_x | \Phi_0 \rangle + \sum_{\mu} \langle \Phi_0 (1 + \Lambda) | [\bar{\mu}_x, \tau_{\mu}] | \Phi_0 \rangle \left(\frac{\partial T}{\partial \epsilon_y} \right)_{\mu},\end{aligned}\quad (31)$$

where τ_{μ} is an excitation operator defined as $\tau_{\mu} |\Phi_0\rangle = |\Phi_{\mu}\rangle$ and

$$\bar{\mu}_x = e^{-T} \mu_x e^T. \quad (32)$$

Rather than using the above expression for deriving the programmable expressions, our implementation employs the density-matrix formulation. Term-for-term, Eq. (31) is equivalent to the following:

$$\alpha_{xy}^0 = \frac{d\mu_x^0}{d\epsilon_y} = \sum_{pq} \left(\frac{\partial \gamma_{pq}}{\partial \Lambda} \frac{\partial \Lambda}{\partial \epsilon_y} \right) \mu_{x,pq} + \sum_{pq} \left(\frac{\partial \gamma_{pq}}{\partial T} \frac{\partial T}{\partial \epsilon_y} \right) \mu_{x,pq}. \quad (33)$$

The programmable expressions of partial derivatives of different blocks of CCSD density matrix are given in the [supplementary material](#).

The above formulation requires the first-order response of the CCSD amplitudes ($\frac{\partial T}{\partial \epsilon_y}$), consistent with the $2n + 1$ rule. Although the first-order response of Lagrange multipliers ($\frac{\partial \Lambda}{\partial \epsilon_y}$) is present in the above equation, it is guaranteed to be unnecessary for the second-order property by the $2n + 2$ rule. The reformulation of the term involving the $\frac{\partial \Lambda}{\partial \epsilon_y}$ -amplitudes in terms of Λ -, T -, and $\frac{\partial T}{\partial \epsilon_y}$ -amplitudes is presented in Section II.

1. First-order response of CCSD T-amplitudes: $\frac{\partial T}{\partial \epsilon_y}$

The first-order cluster amplitudes, $\frac{\partial T}{\partial \epsilon_y}$, can be computed by taking the derivative of the coupled-cluster equation (Eq. (7)) and iteratively solving the nonhomogenous system of linear equations in $\frac{\partial T}{\partial \epsilon_y}$ -amplitudes as follows:

$$-\langle \Phi_{\mu} | \bar{\mu}_y | \Phi_0 \rangle + \sum_{\nu} \langle \Phi_{\mu} | [\bar{H}, \tau_{\nu}] | \Phi_0 \rangle \left(\frac{\partial T}{\partial \epsilon_y} \right)_{\nu} = 0, \quad (34)$$

where μ and ν denote the level of excitation (single or double in CCSD). In our implementation, $\frac{\partial T}{\partial \epsilon_y}$ -amplitudes are computed during the calculation of the CCSD polarizabilities and stored for subsequent calculations of the excited-state polarizabilities. The programmable expression for the response intermediate (first term) in Eq. (34) is provided in the [supplementary material](#). The second term is computed by replacing the R_1 - and R_2 -amplitudes with $\left(\frac{\partial T}{\partial \epsilon_y} \right)_1$ - and $\left(\frac{\partial T}{\partial \epsilon_y} \right)_2$ -amplitudes in the EOM-CCSD σ -vector code.

2. Reformulation of the term involving the first-order response of the CCSD Λ -amplitudes ($\frac{\partial \Lambda}{\partial \epsilon_y}$)

When the CCSD Lagrangian is stationary with respect to the cluster amplitudes T , its first derivative with respect to T -amplitudes is zero and gives rise to the Λ -equations:

$$\frac{d\mathcal{L}}{dT} = \sum_{\nu} \langle \Phi_0 (1 + \Lambda) | [\bar{H}, \tau_{\nu}] | \Phi_0 \rangle \left(\frac{\partial T}{\partial T} \right)_{\nu} = 0, \quad (35)$$

$$\langle \Phi_0 (1 + \Lambda) | [\bar{H}, \tau_{\nu}] | \Phi_0 \rangle = 0. \quad (36)$$

Taking the first derivative of Eq. (36) with respect to the electric-field perturbation, we obtain the following:

$$\begin{aligned}&\langle \Phi_0 \frac{\partial \Lambda}{\partial \epsilon_y} | [\bar{H}, \tau_{\nu}] | \Phi_0 \rangle \\ &- \langle \Phi_0 (1 + \Lambda) | [\bar{\mu}_y, \tau_{\nu}] | \Phi_0 \rangle \\ &+ \sum_{\rho} \langle \Phi_0 (1 + \Lambda) | [[\bar{H}, \tau_{\rho}], \tau_{\nu}] | \Phi_0 \rangle \left(\frac{\partial T}{\partial \epsilon_y} \right)_{\rho} = 0\end{aligned}\quad (37)$$

and

$$\begin{aligned}&- \sum_{\mu} \langle \Phi_0 \frac{\partial \Lambda}{\partial \epsilon_y} | \Phi_{\mu} \rangle \langle \Phi_{\mu} | \bar{H} - E_0 | \Phi_{\nu} \rangle \\ &- \langle \Phi_0 (1 + \Lambda) | [\bar{\mu}_y, \tau_{\nu}] | \Phi_0 \rangle \\ &+ \sum_{\rho} \langle \Phi_0 (1 + \Lambda) | [[\bar{H}, \tau_{\rho}], \tau_{\nu}] | \Phi_0 \rangle \left(\frac{\partial T}{\partial \epsilon_y} \right)_{\rho}.\end{aligned}\quad (38)$$

The left-hand side of the Λ -equation (Eq. (36)) is the CCSD $\tilde{\sigma}$ -vector (similar to the EOM-CCSD $\tilde{\sigma}$ -vectors):

$$\tilde{\sigma}_{\nu}^0 = 0. \quad (39)$$

Term-for-term, Eq. (38) is the same as the following equation obtained by taking the first derivative of Eq. (39):

$$-\frac{\partial \tilde{\sigma}_{\nu}^0}{\partial \Lambda} \frac{\partial \Lambda}{\partial \epsilon_y} = \frac{\partial \tilde{\sigma}_{\nu}^0}{\partial \epsilon_y} + \frac{\partial \tilde{\sigma}_{\nu}^0}{\partial T} \frac{\partial T}{\partial \epsilon_y}. \quad (40)$$

Using Eqs. (34), (38), and (40), the term involving the first-order response of CCSD Λ -amplitudes can now be re-written as follows:

$$\begin{aligned}&\langle \Phi_0 \frac{\partial \Lambda}{\partial \epsilon_y} | \bar{\mu}_x | \Phi_0 \rangle \\ &= \sum_{\mu\nu\rho} \langle \Phi_0 \frac{\partial \Lambda}{\partial \epsilon_y} | \Phi_{\mu} \rangle \langle \Phi_{\mu} | \bar{H} - E_0 | \Phi_{\nu} \rangle \\ &\times \langle \Phi_{\nu} | [\bar{H} - E_0]^{-1} | \Phi_{\rho} \rangle \langle \Phi_{\rho} | \bar{\mu}_x | \Phi_0 \rangle \\ &= \sum_{\mu\nu} \langle \Phi_0 \frac{\partial \Lambda}{\partial \epsilon_y} | \Phi_{\mu} \rangle \langle \Phi_{\mu} | \bar{H} - E_0 | \Phi_{\nu} \rangle \langle \Phi_{\nu} | \frac{\partial T}{\partial \epsilon_x} \Phi_0 \rangle \\ &= \sum_{\nu} \langle \Phi_0 (1 + \Lambda) | [\bar{\mu}_y, \tau_{\nu}] | \Phi_0 \rangle \left(\frac{\partial T}{\partial \epsilon_x} \right)_{\nu} \\ &- \sum_{\rho\nu} \langle \Phi_0 (1 + \Lambda) | [[\bar{H}, \tau_{\rho}], \tau_{\nu}] | \Phi_0 \rangle \left(\frac{\partial T}{\partial \epsilon_y} \right)_{\rho} \left(\frac{\partial T}{\partial \epsilon_x} \right)_{\nu} \\ &= - \sum_{\nu} \left(\frac{\partial \tilde{\sigma}_{\nu}^0}{\partial \epsilon_y} + \frac{\partial \tilde{\sigma}_{\nu}^0}{\partial T} \frac{\partial T}{\partial \epsilon_y} \right) \left(\frac{\partial T}{\partial \epsilon_x} \right)_{\nu}.\end{aligned}\quad (41)$$

3. Final programmable expression for CCSD static polarizability

Combining Eqs. (33) and (41), the expression for the CCSD static polarizability assumes the following form:

$$\begin{aligned}\alpha_{xy}^0 &= - \sum_{\nu} \left(\frac{\partial \tilde{\sigma}_{\nu}^0}{\partial \epsilon_y} + \frac{\partial \tilde{\sigma}_{\nu}^0}{\partial T} \frac{\partial T}{\partial \epsilon_y} \right) \left(\frac{\partial T}{\partial \epsilon_x} \right)_{\nu} \\ &+ \sum_{pq} \left(\frac{\partial \gamma_{pq}}{\partial T} \frac{\partial T}{\partial \epsilon_y} \right) (\mu_x)_{pq}.\end{aligned}\quad (42)$$

D. EOM-(EE/SF)-CCSD Lagrangian and dipole moment

The EOM-CC Lagrangian for state k depends on the T -, R -, L -, and Z -amplitudes:

$$\begin{aligned} \mathcal{L}^k(T, L^k, R^k, Z^k) &= \langle \Phi_0 | L^k | e^{-T} H e^T | R^k \Phi_0 \rangle + \sum_{\mu=1}^2 z_{\mu}^k \langle \Phi_{\mu} | e^{-T} H e^T | \Phi_0 \rangle \\ &= \langle \Phi_0 | L^k | e^{-T} H e^T | R^k \Phi_0 \rangle + \langle \Phi_0 | Z^k | e^{-T} H e^T | \Phi_0 \rangle, \quad (43) \end{aligned}$$

where the first term is the EOM-CC energy for state k , the second term represents the constraints imposed by the CC equations (Eq. (7)), and Z^k are the amplitude-response Lagrange multipliers. In the rest of this section, we drop index k .

This Lagrangian can be made stationary with respect to all parameters, meaning $\frac{\partial \mathcal{L}}{\partial T}$, $\frac{\partial \mathcal{L}}{\partial L}$, $\frac{\partial \mathcal{L}}{\partial R}$, and $\frac{\partial \mathcal{L}}{\partial Z}$ are all equal to zero. Then, the first derivative of the EOM-CCSD energy (which equals the first derivative of the Lagrangian) is given by the partial derivative of the Lagrangian,

$$\frac{dE}{d\epsilon} = \frac{d\mathcal{L}}{d\epsilon} = \frac{\partial \mathcal{L}}{\partial \epsilon} + \frac{\partial \mathcal{L}}{\partial T} \frac{\partial T}{\partial \epsilon} + \frac{\partial \mathcal{L}}{\partial R} \frac{\partial R}{\partial \epsilon} + \frac{\partial \mathcal{L}}{\partial L} \frac{\partial L}{\partial \epsilon} + \frac{\partial \mathcal{L}}{\partial Z} \frac{\partial Z}{\partial \epsilon} = \frac{\partial \mathcal{L}}{\partial \epsilon} = \langle \Phi_0 | L | e^{-T} \frac{\partial H}{\partial \epsilon} e^T | R \Phi_0 \rangle + \langle \Phi_0 | Z | e^{-T} \frac{\partial H}{\partial \epsilon} e^T | \Phi_0 \rangle. \quad (44)$$

Thus, the negative of the first derivative of the EOM-CCSD energy with respect to the electric-field perturbation equals the dipole moment of EOM state k and is given by

$$\mu_x = \langle \Phi_0 | L | e^{-T} \mu_x e^T | R \Phi_0 \rangle + \langle \Phi_0 | Z | e^{-T} \mu_x e^T | \Phi_0 \rangle, \quad (45)$$

where the two terms are the expectation-value and the amplitude-response contributions, respectively. Note that the orbital-response contribution has been omitted. Eq. (45) can be written using density matrices as

$$\mu_x = \sum_{pq} \gamma'_{pq} \mu_{x,pq} + \sum_{pq} \gamma''_{pq} \mu_{x,pq}, \quad (46)$$

where γ'_{pq} is the unrelaxed EOM-CC one-particle density matrix and γ''_{pq} is the amplitude response part. The expressions for the different blocks of the EOM-CCSD density matrices (γ'_{pq} and γ''_{pq}) are given in Ref. 38 and also in the supplementary material.

E. EOM-(EE/SF)-CCSD static polarizabilities as analytic derivatives

The EOM-CCSD static polarizabilities are given by the negative of the second derivatives of the EOM-CCSD energy with respect to two electric-field perturbations or, equivalently, by the first derivative of the dipole moment with respect to an electric-field perturbation as follows:

$$\begin{aligned} \alpha_{xy} &= \frac{d\mu_x}{d\epsilon_y} \\ &= \langle \Phi_0 | \frac{\partial L}{\partial \epsilon_y} | \bar{\mu}_x | R \Phi_0 \rangle + \sum_{\mu} \langle \Phi_0 | L | [\bar{\mu}_x, \tau_{\mu}] | R \Phi_0 \rangle \left(\frac{\partial T}{\partial \epsilon_y} \right)_{\mu} \\ &\quad + \langle \Phi_0 | L | [\bar{\mu}_x] | \frac{\partial R}{\partial \epsilon_y} \Phi_0 \rangle + \sum_{\mu} \langle \Phi_0 | Z | [\bar{\mu}_x, \tau_{\mu}] | \Phi_0 \rangle \left(\frac{\partial T}{\partial \epsilon_y} \right)_{\mu} \\ &\quad + \langle \Phi_0 | \frac{\partial Z}{\partial \epsilon_y} | \bar{\mu}_x | \Phi_0 \rangle. \quad (47) \end{aligned}$$

Term-for-term, Eq. (47) is the same as the following equation, obtained by taking the derivative of Eq. (46) with respect to

the electric-field perturbation:

$$\begin{aligned} \alpha_{xy} &= \frac{d\mu_x}{d\epsilon_y} \\ &= \sum_{pq} \left(\frac{\partial \gamma'_{pq}}{\partial L} \frac{\partial L}{\partial \epsilon_y} \right) \mu_{x,pq} + \sum_{pq} \left(\frac{\partial \gamma'_{pq}}{\partial T} \frac{\partial T}{\partial \epsilon_y} \right) \mu_{x,pq} \\ &\quad + \sum_{pq} \left(\frac{\partial \gamma'_{pq}}{\partial R} \frac{\partial R}{\partial \epsilon_y} \right) \mu_{x,pq} + \sum_{pq} \left(\frac{\partial \gamma''_{pq}}{\partial T} \frac{\partial T}{\partial \epsilon_y} \right) \mu_{x,pq} \\ &\quad + \sum_{pq} \left(\frac{\partial \gamma''_{pq}}{\partial Z} \frac{\partial Z}{\partial \epsilon_y} \right) \mu_{x,pq}. \quad (48) \end{aligned}$$

The programmable expressions of the partial derivatives of different blocks of the EOM-CCSD one-particle density matrices (γ'_{pq} and γ''_{pq}) are provided in the supplementary material.

Eq. (47) follows the asymmetric formulation of the second-order property of the EOM-CCSD wave functions presented in Ref. 36. The above formulation requires the first-order responses of the T - and R -amplitudes, consistent with the $2n+1$ rule. Although the first-order responses of the L - and Z -amplitudes are present in the first and last terms of Eqs. (47) and (48), these are guaranteed to be unnecessary for the second-order property by the $2n+2$ rule. The symmetric formulation presented in Ref. 36 satisfies the $2n+2$ rule for the L - and Z -amplitudes. Our implementation has a mixed symmetric-asymmetric formulation, wherein the $2n+2$ rule is satisfied for the Z -amplitudes, but not for the L -amplitudes. We reformulate the term involving the $\frac{\partial Z}{\partial \epsilon_y}$ -amplitudes in terms of Z -, T -, L -, R -, $\frac{\partial T}{\partial \epsilon_y}$ -, $\frac{\partial L}{\partial \epsilon_y}$ -, and $\frac{\partial R}{\partial \epsilon_y}$ -amplitudes (presented in Section II E 3). Note that the static polarizabilities derived as analytic second derivatives are size-extensive.

1. First-order response of EOM-CCSD R- and L-amplitudes: $\frac{\partial R}{\partial \epsilon_y}$ and $\frac{\partial L}{\partial \epsilon_y}$

The EOM-CCSD right- and left-eigenvalue equations, Eqs. (9) and (10), can be equivalently expressed as

$$\langle \Phi_{\mu} | [\bar{H}, R] | \Phi_0 \rangle = \Omega \langle \Phi_{\mu} | R \Phi_0 \rangle, \quad (49)$$

$$\langle \Phi_0 | L | [\bar{H}, \tau_{\mu}] | \Phi_0 \rangle = \Omega \langle \Phi_0 | L | \Phi_{\mu} \rangle. \quad (50)$$

$\frac{\partial R}{\partial \epsilon_y}$ - and $\frac{\partial L}{\partial \epsilon_y}$ -amplitudes can be evaluated by taking the first derivative of Eqs. (49) and (50) with respect to the electric-field perturbation and then iteratively solving the nonhomogenous systems of linear equations in terms of $\frac{\partial R}{\partial \epsilon_y}$ - and $\frac{\partial L}{\partial \epsilon_y}$ -amplitudes as follows:

$$\begin{aligned} \langle \Phi_\mu | \bar{H} - E | \frac{\partial R}{\partial \epsilon_y} \Phi_0 \rangle &= \left(\langle \phi_\mu | [\bar{\mu}_y, R] | \Phi_0 \rangle - (\mu_y^k - \mu_y^0) \langle \Phi_\mu | R \Phi_0 \rangle \right) \\ &\quad - \sum_\nu \langle \Phi_\mu | [(\bar{H}, \tau_\nu], R] | \Phi_0 \rangle \left(\frac{\partial T}{\partial \epsilon_y} \right)_\nu; \end{aligned} \quad (51)$$

$$\begin{aligned} \langle \Phi_0 | \frac{\partial L}{\partial \epsilon_y} | \bar{H} - E | \Phi_\mu \rangle &= \left(\langle \Phi_0 L | [\bar{\mu}_y, \tau_\mu] | \Phi_0 \rangle - (\mu_y^k - \mu_y^0) \langle \Phi_0 L | \Phi_\mu \rangle \right) \\ &\quad - \sum_\nu \langle \Phi_0 L | [(\bar{H}, \tau_\nu], \tau_\mu] | \Phi_0 \rangle \left(\frac{\partial T}{\partial \epsilon_y} \right)_\nu, \end{aligned} \quad (52)$$

where μ_y^k is scalar x -, y -, or z -component of the dipole moment of EOM-CCSD state k . In terms of the EOM-CCSD σ - and $\tilde{\sigma}$ -vectors, the right and left-eigenvalue equations can be written as

$$\sigma_\mu - \Omega R_\mu = 0; \quad (53)$$

$$\tilde{\sigma}_\mu - L_\mu \Omega = 0. \quad (54)$$

In terms of the partial derivatives of σ_μ and $\tilde{\sigma}_\mu$, Eqs. (51) and (52) are the same as

$$\langle \Phi_\mu | \bar{H} - E | \frac{\partial R}{\partial \epsilon_y} \Phi_0 \rangle = - \left(\frac{\partial \sigma_\mu}{\partial \epsilon_y} - \frac{\partial \Omega}{\partial \epsilon_y} R_\mu \right) - \frac{\partial \sigma_\mu}{\partial T} \frac{\partial T}{\partial \epsilon_y}; \quad (55)$$

$$\langle \Phi_0 | \frac{\partial L}{\partial \epsilon_y} | \bar{H} - E | \Phi_\mu \rangle = - \left(\frac{\partial \tilde{\sigma}_\mu}{\partial \epsilon_y} - L_\mu \frac{\partial \Omega}{\partial \epsilon_y} \right) - \frac{\partial \tilde{\sigma}_\mu}{\partial T} \frac{\partial T}{\partial \epsilon_y}. \quad (56)$$

Eqs. (55) and (56) are solved iteratively using the DIIS procedure for calculating the $\frac{\partial R}{\partial \epsilon_y}$ - and $\frac{\partial L}{\partial \epsilon_y}$ -amplitudes, respectively. The programmable expressions for the partial derivatives of the EOM-CCSD σ - and $\tilde{\sigma}$ -intermediates and the setup of the iterative DIIS procedure are given in the [supplementary material](#).

2. Removal of singularities in response equations

The convergence of the first-order EOM-CCSD left and right amplitudes could become numerically unstable due to the small diagonal components of the $[\bar{H} - E_k]$ matrix. Since

Eqs. (58) and (57) for the first-order responses of the EOM-CCSD amplitudes are valid (owing to the EOM-CCSD eigenvalue equations), these divergences are trivially avoided by explicitly working in the biorthogonal space of the target state, k :

$$\begin{aligned} \langle \Phi_\mu | \bar{H} - E_k | \frac{\partial R^k}{\partial \epsilon_y} \Phi_0 \rangle &= \langle \Phi_\mu | \left[1 - |R^k \Phi_0\rangle \langle \Phi_0 L^k| \right] [\bar{H} - E_k] \\ &\quad \times \left[1 - |R^k \Phi_0\rangle \langle \Phi_0 L^k| \right] | \frac{\partial R^k}{\partial \epsilon_y} \Phi_0 \rangle; \end{aligned} \quad (57)$$

$$\begin{aligned} \langle \Phi_0 | \frac{\partial L^k}{\partial \epsilon_y} | \bar{H} - E_k | \Phi_\mu \rangle &= \langle \Phi_0 | \frac{\partial L^k}{\partial \epsilon_y} | \left[1 - |R^k \Phi_0\rangle \langle \Phi_0 L^k| \right] \\ &\quad \times [\bar{H} - E_k] \left[1 - |R^k \Phi_0\rangle \langle \Phi_0 L^k| \right] | \Phi_\mu \rangle, \end{aligned} \quad (58)$$

where $\left[1 - |R^k \Phi_0\rangle \langle \Phi_0 L^k| \right]$ projects out state k from the $[\bar{H} - E_k]$ matrix. Although the programmable expressions of the response equations, Eqs. (55) and (56), employ the same left-hand sides as Eqs. (57) and (58), respectively, the preconditioners in the iterative DIIS procedure correspond to the right-hand side of Eqs. (57) and (58), which give numerically stable convergence.

3. Reformulation of the term involving the first-order response of the Z-amplitudes ($\frac{\partial Z}{\partial \epsilon_y}$)

The term involving the first-order response of the Lagrange multipliers Z can be rearranged as follows:

$$\begin{aligned} \langle \Phi_0 | \frac{\partial Z}{\partial \epsilon_y} | \bar{\mu}_x | \Phi_0 \rangle &= \sum_{\rho, \mu, \nu} \langle \Phi_0 | \frac{\partial Z}{\partial \epsilon_y} | \Phi_\rho \rangle \langle \Phi_\rho | \bar{H} - E_{CC} | \Phi_\mu \rangle \langle \Phi_\mu | \\ &\quad \times [\bar{H} - E_{CC}]^{-1} | \Phi_\nu \rangle \langle \Phi_\nu | \bar{\mu}_x | \Phi_0 \rangle \\ &= \sum_{\rho, \mu} \langle \Phi_0 | \frac{\partial Z}{\partial \epsilon_y} | \Phi_\rho \rangle \langle \Phi_\rho | \bar{H} - E_{CC} | \Phi_\mu \rangle \\ &\quad \times \langle \Phi_\mu | \frac{\partial T}{\partial \epsilon_x} \Phi_0 \rangle, \end{aligned} \quad (59)$$

where ρ , μ , and ν correspond to single or double excitation levels and the expression for the first-order cluster amplitudes, is given in Section III E 1. $\langle \Phi_0 | \frac{\partial Z}{\partial \epsilon_y} | \Phi_\rho \rangle \langle \Phi_\rho | \bar{H} - E_{CC} | \Phi_\mu \rangle$ can be evaluated by taking the first derivative of the zero-order amplitude response equation of EOM-CCSD as follows:

$$\langle \Phi_0 Z | \bar{H} - E_0 | \Phi_\mu \rangle = - \langle \Phi_0 L | [\bar{H}, \tau_\mu] | R \Phi_0 \rangle, \quad (60)$$

$$\begin{aligned} \langle \Phi_0 | \frac{\partial Z}{\partial \epsilon_y} | \bar{H} - E_0 | \Phi_\mu \rangle &- \langle \Phi_0 Z | \bar{\mu}_y - \mu_y^0 | \Phi_\mu \rangle + \sum_\nu \langle \Phi_0 Z | [\bar{H}, \tau_\nu] | \Phi_\mu \rangle \left(\frac{\partial T}{\partial \epsilon_y} \right)_\nu \\ &= - \langle \Phi_0 | \frac{\partial L}{\partial \epsilon_y} | [\bar{H}, \tau_\mu] | R \Phi_0 \rangle - \langle \Phi_0 L | [\bar{H}, \tau_\mu] | \frac{\partial R}{\partial \epsilon_y} \Phi_0 \rangle \\ &\quad + \langle \Phi_0 L | [\bar{\mu}_y, \tau_\mu] | R \Phi_0 \rangle - \sum_\nu \langle \Phi_0 L | [\bar{H}, \tau_\mu], \tau_\nu] | R \Phi_0 \rangle \left(\frac{\partial T}{\partial \epsilon_y} \right)_\nu. \end{aligned} \quad (61)$$

The left-hand side of Eq. (60) is the EOM-CCSD $\tilde{\sigma}_\mu$ -vector computed by replacing the L -amplitudes by the Z -amplitudes. The right-hand side of Eq. (60) is denoted by $-\xi_\mu$ so that Eq. (60) can be written as

$$Z \tilde{\sigma}_\mu = -\xi_\mu. \quad (62)$$

Term-for-term, Eq. (61) is same as the following expression in terms of the partial derivatives of ${}^Z\tilde{\sigma}_\mu$ and ξ_μ :

$$\langle \Phi_0 \frac{\partial Z}{\partial \epsilon_y} | \bar{H} - E_{CC} | \Phi_\mu \rangle + \frac{\partial ({}^Z\tilde{\sigma}_\mu)}{\partial \epsilon_y} + \frac{\partial ({}^Z\tilde{\sigma}_\mu)}{\partial T} \frac{\partial T}{\partial \epsilon_y} = - \frac{\partial \xi_\mu}{\partial L} \frac{\partial L}{\partial \epsilon_y} - \frac{\partial \xi_\mu}{\partial R} \frac{\partial R}{\partial \epsilon_y} - \frac{\partial \xi_\mu}{\partial \epsilon_y} - \frac{\partial \xi_\mu}{\partial T} \frac{\partial T}{\partial \epsilon_y}. \quad (63)$$

After insertion of the identity operator ($\sum_\rho |\Phi_\rho\rangle\langle\Phi_\rho| = 1$) in the first term, the above equation can be rearranged as follows:

$$\sum_\rho \langle \Phi_0 \frac{\partial Z}{\partial \epsilon_y} | \Phi_\rho \rangle \langle \Phi_\rho | \bar{H} - E_{CC} | \Phi_\mu \rangle = - \frac{\partial ({}^Z\tilde{\sigma}_\mu)}{\partial \epsilon_y} - \frac{\partial ({}^Z\tilde{\sigma}_\mu)}{\partial T} \frac{\partial T}{\partial \epsilon_y} - \frac{\partial \xi_\mu}{\partial L} \frac{\partial L}{\partial \epsilon_y} - \frac{\partial \xi_\mu}{\partial R} \frac{\partial R}{\partial \epsilon_y} - \frac{\partial \xi_\mu}{\partial \epsilon_y} - \frac{\partial \xi_\mu}{\partial T} \frac{\partial T}{\partial \epsilon_y}, \quad (64)$$

where only the terms involving ρ corresponding to single or double excitation survive because $\frac{\partial Z}{\partial \epsilon_y}$ -amplitudes can only connect singles and doubles excitations to Φ_0 . Combining Eqs. (59) and (64), the reformulated expression for $\langle \Phi_0 \frac{\partial Z}{\partial \epsilon_y} | \frac{\partial \bar{H}}{\partial \epsilon_x} | \Phi_0 \rangle$ becomes

$$\langle \Phi_0 \frac{\partial Z}{\partial \epsilon_y} | \frac{\partial \bar{H}}{\partial \epsilon_x} | \Phi_0 \rangle = - \sum_\mu \left(\frac{\partial ({}^Z\tilde{\sigma}_\mu)}{\partial \epsilon_y} + \frac{\partial ({}^Z\tilde{\sigma}_\mu)}{\partial T} \frac{\partial T}{\partial \epsilon_y} \right) \left(\frac{\partial T}{\partial \epsilon_x} \right)_\mu - \sum_\mu \left(\frac{\partial \xi_\mu}{\partial L} \frac{\partial L}{\partial \epsilon_y} + \frac{\partial \xi_\mu}{\partial R} \frac{\partial R}{\partial \epsilon_y} + \frac{\partial \xi_\mu}{\partial \epsilon_y} + \frac{\partial \xi_\mu}{\partial T} \frac{\partial T}{\partial \epsilon_y} \right) \left(\frac{\partial T}{\partial \epsilon_x} \right)_\mu. \quad (65)$$

4. Final expression for EOM-CCSD polarizability

Combining Eqs. (48) and (65), the final expression for the xy -component of the EOM-CCSD polarizability is given as follows:

$$\alpha_{xy} = \sum_{pq} \left(\frac{\partial \gamma'_{pq}}{\partial L} \frac{\partial L}{\partial \epsilon_y} \right) (\mu_x)_{pq} + \sum_{pq} \left(\frac{\partial \gamma'_{pq}}{\partial T} \frac{\partial T}{\partial \epsilon_y} \right) (\mu_x)_{pq} + \sum_{pq} \left(\frac{\partial \gamma'_{pq}}{\partial R} \frac{\partial R}{\partial \epsilon_y} \right) (\mu_x)_{pq} + \sum_{pq} \left(\frac{\partial \gamma''_{pq}}{\partial T} \frac{\partial T}{\partial \epsilon_y} \right) (\mu_x)_{pq} \\ - \sum_\mu \left(\frac{\partial ({}^Z\tilde{\sigma}_\mu)}{\partial \epsilon_y} + \frac{\partial ({}^Z\tilde{\sigma}_\mu)}{\partial T} \frac{\partial T}{\partial \epsilon_y} \right) \left(\frac{\partial T}{\partial \epsilon_x} \right)_\mu - \sum_\mu \left(\frac{\partial \xi_\mu}{\partial L} \frac{\partial L}{\partial \epsilon_y} + \frac{\partial \xi_\mu}{\partial R} \frac{\partial R}{\partial \epsilon_y} + \frac{\partial \xi_\mu}{\partial \epsilon_y} + \frac{\partial \xi_\mu}{\partial T} \frac{\partial T}{\partial \epsilon_y} \right) \left(\frac{\partial T}{\partial \epsilon_x} \right)_\mu. \quad (66)$$

F. Implementation of polarizabilities as analytic derivatives: Summary of the algorithm

All equations are implemented in the Q-Chem electronic structure package^{60,61} using libtensor library.⁶² The CCSD and EOM-CCSD polarizabilities are computed as follows:

- Once the CCSD T - and Λ -equations are solved, the intermediates in Eq. (34) needed for calculating the $\frac{\partial T}{\partial \epsilon}$ -amplitudes iteratively are computed and stored. Three response equations corresponding to the three components of $\frac{\partial T}{\partial \epsilon}$ are solved by the DIIS procedure given in the [supplementary material](#) (Section II).
- The partial derivatives of the CCSD $\tilde{\sigma}$ -intermediates ([supplementary material](#) Section IV) and the partial derivatives of the CCSD one-particle density matrix ([supplementary material](#) Section III) are computed, followed by the calculation of the CCSD polarizability tensor according to Eq. (42).
- The $\frac{\partial T}{\partial \epsilon}$ -amplitudes and the intermediates required for further calculations are stored for the subsequent use in the EOM-CCSD polarizability calculation.
- The EOM right- and left-amplitudes and energies are computed as usual.
- The amplitude response (Z -amplitudes) and orbital relaxation are computed for the first-order state properties such as dipole moments.

- Necessary intermediates, such as the partial derivatives of the σ - and $\tilde{\sigma}$ -intermediates ([supplementary material](#) Sections VII and V) in Eqs. (55) and (56), are computed followed by the DIIS calculations of the $\frac{\partial R}{\partial \epsilon}$ - and $\frac{\partial L}{\partial \epsilon}$ -amplitudes (two sets of three response equations solved according to the DIIS procedure in [supplementary material](#), Sections VIII and VI).
- Partial derivatives of the EOM-CCSD density matrices (γ' and γ'') and the ${}^Z\tilde{\sigma}$ - and ξ -intermediates required in Eq. (66) are computed ([supplementary material](#), Sections IX and X).
- All components of the EOM-CCSD polarizabilities are computed and collected to form the polarizability tensor according to Eq. (66).

G. Static polarizabilities as expectation values

In contrast to the static polarizabilities calculated as second derivatives of the energies, the expectation-value approach involves using approximate EOM-CCSD wave functions and energies in the sum-over-states polarizability expression (derived for exact states) in Eq. (2). The expectation-value approach has been shown to yield the CCSD polarizabilities similar in quality to those obtained with the CCSD response theory,⁵ but the results are not size-extensive. As demonstrated by the derivation that follows, significantly fewer response equations need to be solved within the expectation-value approach (in addition to the fewer intermediates that

need to be stored and the fewer floating-point operations). Motivated by the elegance of this CI-like formalism and by its computational-cost advantages, we have employed this approach for computing two-photon absorption cross sections between the ground- and excited-states in closed-shell systems, with accuracy similar to that of the CCSD response

theory.³¹ This approach is also employed for computing the spin-orbit couplings for the EOM-CCSD wave functions in Q-Chem.³³

After plugging the EOM-CCSD (or CCSD) wave functions and energies into Eq. (2), we invoke the identity operator in the Fock space ($\sum_I |\Phi_I\rangle\langle\Phi_I| = 1$) as follows:

$$\begin{aligned} \alpha_{xy}(0) &= \mathcal{P}_{xy}^+ \sum_{n \neq k} \frac{\langle \Phi_0 L^k e^{-T} | \mu_x | e^T R^n \Phi_0 \rangle \langle \Phi_0 L^n e^{-T} | \mu_y | e^T R^k \Phi_0 \rangle}{E_n - E_k} \\ &= \mathcal{P}_{xy}^+ \sum_{n \neq k} \sum_{IJ} \langle \Phi_0 L^k e^{-T} | \mu_x | e^T \Phi_I \rangle \frac{\langle \Phi_I | R^n \Phi_0 \rangle \langle \Phi_0 L^n | \Phi_J \rangle}{E_n - E_k} \langle \Phi_J e^{-T} | \mu_y | e^T R^k \Phi_0 \rangle \\ &= \mathcal{P}_{xy}^+ \sum_{IJ} \langle \Phi_0 L^k | \bar{\mu}_x | \Phi_I \rangle \langle \Phi_I | [1 - |R^k \Phi_0\rangle\langle\Phi_0 L^k|] \\ &\quad ([1 - |R^k \Phi_0\rangle\langle\Phi_0 L^k|] [\bar{H} - E_k] [1 - |R^k \Phi_0\rangle\langle\Phi_0 L^k|])^{-1} |\Phi_J\rangle \langle\Phi_J| \bar{\mu}_y |R^k \Phi_0\rangle, \end{aligned} \quad (67)$$

where Φ_I 's denote the reference, singly, and doubly excited Slater determinants. The last step follows from the following identity:

$$([1 - |R^k \Phi_0\rangle\langle\Phi_0 L^k|] [\bar{H} - E_k] [1 - |R^k \Phi_0\rangle\langle\Phi_0 L^k|]) \sum_{n \neq k} \frac{\langle \Phi_I | R^n \Phi_0 \rangle \langle \Phi_0 L^n | \Phi_J \rangle}{E_n - E_k} = \langle \Phi_I | [1 - |R^k \Phi_0\rangle\langle\Phi_0 L^k|] |\Phi_J\rangle. \quad (68)$$

Thus, Eq. (67) becomes

$$\begin{aligned} \alpha_{xy}(0) &= \mathcal{P}_{xy}^+ \sum_{IJM} [\tilde{D}_x^k]_I [1 - |R^k \Phi_0\rangle\langle\Phi_0 L^k|]_{IM} \left(([1 - |R^k \Phi_0\rangle\langle\Phi_0 L^k|] [\bar{H} - E_k] [1 - |R^k \Phi_0\rangle\langle\Phi_0 L^k|])^{-1} \right)_{MJ} [D_y^k]_J \\ &= \mathcal{P}_{xy}^+ \sum_{JM} [\tilde{D}_x^{k,eff}]_M \left(([1 - |R^k \Phi_0\rangle\langle\Phi_0 L^k|] [\bar{H} - E_k] [1 - |R^k \Phi_0\rangle\langle\Phi_0 L^k|])^{-1} \right)_{MJ} [D_y^k]_J \\ &= \mathcal{P}_{xy}^+ \sum_J [\tilde{X}_x^k]_J [D_y^k]_J, \end{aligned} \quad (69)$$

where the \tilde{D} -, D -, and \tilde{D}^{eff} -intermediates are

$$[\tilde{D}_x^k]_I = \langle \Phi_0 L^k | \bar{\mu}_x | \Phi_I \rangle, \quad (70)$$

$$[D_y^k]_J = \langle \Phi_J | \bar{\mu}_y | R^k \Phi_0 \rangle, \quad (71)$$

$$[\tilde{D}_x^{k,eff}]_M = \sum_I [\tilde{D}_x^k]_I [1 - |R^k \Phi_0\rangle\langle\Phi_0 L^k|]_{IM}. \quad (72)$$

The programmable expressions for the intermediates, \tilde{D} and D , are provided in Ref. 31. The response vectors \tilde{X} are computed iteratively, by solving the following response equation:

$$\tilde{X}_x^k ([1 - |R^k \Phi_0\rangle\langle\Phi_0 L^k|] [\bar{H} - E_k] [1 - |R^k \Phi_0\rangle\langle\Phi_0 L^k|]) = \tilde{D}_x^{k,eff}. \quad (73)$$

For static polarizabilities, only three such response equations (for x -, y - and z -components) are solved in the expectation-value approach for each state (ground or excited). While the CCSD static polarizabilities as second derivatives of electric-field perturbations also require three response equations to be solved (for first-order response amplitudes of T for x -, y - and z -perturbations), the excited-state static polarizabilities require seven additional response equations to be solved (one response equation for the zero-order Z -amplitudes plus three each for the first-order response amplitudes of L and R) in our formulation.

III. COMPUTATIONAL DETAILS

The Cartesian geometries of all the systems studied in this paper are given in the [supplementary material](#). All calculations were performed with the Q-Chem electronic structure package.^{60,61} The reported polarizability components and symmetry labels of the electronic states and MOs correspond to the standard molecular orientation used in Q-Chem, which differs for some irreducible representations from the Mulliken convention.^{63,64}

To validate our implementation against available CCSD response-theory data in Ref. 20, we consider lowest singlet excited states of s-tetrazine and pyrimidine. We used the same structures and POL [5s3p2d/3s2p] basis of Sadlej⁶⁵ with core orbitals frozen. The molecules are oriented as follows: pyrimidine is in xz -plane (z -axis is the C_2 -axis) and s-tetrazine is in xy -plane (with the x -axis passing through the carbon and hydrogen atoms). Note that these orientations are different from those reported in Ref. 20. For pyrimidine, Ref. 20 has the molecule in the xy -plane with the y -axis as the C_2 -axis. Consequently, our α_{yy} and α_{zz} , as well as B_1 and B_2 states, are swapped relative to Ref. 20 for pyrimidine. For s-tetrazine, Ref. 20 has the molecule in the yz -plane with the z -axis passing through the carbon and hydrogen atoms. Consequently, our α_{xx} and α_{zz} , as well as B_{1u} and B_{3u} states, are swapped relative to Ref. 20 for s-tetrazine. For these two benchmark

systems, we also performed finite-field calculations with a step size of 0.0005 a.u. To enable proper comparison with our analytical implementation, wherein the orbital response to the electric-field perturbation is omitted, the electric-field perturbation was switched on only after the Hartree-Fock step so that the molecular orbitals are field-free.

Next, we calculated the static polarizabilities as analytic derivatives with EOM-EE-CCSD/aug-cc-pVDZ for the lowest $n \rightarrow \pi^*$ and $\pi \rightarrow \pi^*$ singlet and triplet states of the uracil molecule. We used the B3LYP/6-311G(2df,2pd) optimized geometry from Ref. 66 for all the ground- and excited-state calculations (the molecule is in the xy -plane). We also calculated EOM-EE-CCSD static polarizabilities for the charge-transfer $\pi \rightarrow \pi^*$ singlet and triplet states of *p*-nitroaniline using the aug-cc-pVDZ and 6-31+G* basis sets. We employed the geometry of *p*-nitroaniline from Ref. 67 (the molecule is in the xz -plane, with the z -axis as the C_2 -axis). To gain an insight into the computed polarizabilities, we performed wave function analysis^{68,69} and calculated natural transition orbitals (NTOs) for uracil and *p*-nitroaniline. NTOs were visualized with Gabedit.⁷⁰

To illustrate the ability of our implementation to calculate static polarizabilities of open-shell diradical systems, we performed EOM-SF-CCSD/cc-pVTZ calculations with high-spin references for prototypical diradicals: methylene and *p*-benzyne. Unrestricted Hartree-Fock method was used for high-spin reference states. For these diradicals, we compare the EOM-SF-CCSD and EOM-EE-CCSD values in order to analyze the effect of correlation treatment on static polarizabilities. For methylene, the polarizabilities were computed for the four lowest electronic states: 3B_2 , 1A_1 , 1B_2 , and 1A_1 . As in our previous benchmarks,^{71–73} we used FCI/TZ2P optimized geometries from Ref. 74. The Mulliken convention⁶³ places methylene in the yz -plane, whereas in Q-Chem calculations, the molecule is in the xz -plane (the z -axis is the C_2 -axis in both cases) such that B_1 states become B_2 states and α_{xx} and α_{yy} are swapped. For the $\sigma\sigma$ *p*-benzyne diradical, we computed polarizabilities of the lowest triplet and singlet electronic states. We employed the SF-CCSD/cc-pVTZ optimized geometries for the 1A_g and $^3B_{2u}$ states from Ref. 73. Compared to the Mulliken convention in which the molecule is in the yz -plane with the z -axis passing through the radical centers, Q-Chem orients this system in the xy -plane with the y -axis passing through the radical centers. Consequently, B_{1u} states in the Mulliken convention show up as B_{2u} states, α_{zz} shows up as α_{yy} , α_{yy} shows up as α_{xx} , and α_{xx} shows up as α_{zz} .

IV. RESULTS AND DISCUSSION

We begin by validating our implementation against the available CCSD response-theory and finite-difference polarizabilities for the lowest singlet excited states of s-tetrazine and pyrimidine molecules. We then proceed to uracil, *p*-nitroaniline, methylene, and *p*-benzyne. In uracil and *p*-nitroaniline, we compare singlet and triplet states. We also compare states of different character, e.g., $n \rightarrow \pi^*$ and $\pi \rightarrow \pi^*$. In methylene, which has weak diradical character, we analyze four lowest electronic states at different geometries. Finally, in *p*-benzyne, we compare two lowest singlet and triplet states.

Before we proceed to the numeric results, let us discuss anticipated trends in polarizabilities. As follows from Eq. (1), polarizability describes how readily the charge distribution (i.e., dipole moment) of the system responds to the electric field. Thus, one can expect that excited states would be more polarizable than the ground states because of the electron-hole separation. States with a larger electron-hole separation (exciton size) and/or more diffuse electron density are expected to have larger polarizabilities. States with strongly ionic character (large permanent dipole) are likely to be less polarizable.

A complementary analysis is based on Eq. (2). Large polarizability can be associated with the presence of nearby dipole-allowed states, i.e., $\alpha_{xx}^0 \sim \left(\frac{<\Psi_0|\mu_x|\Psi_1>}{E_0 - E_1} \right)^2$. Thus, polarizability of a dipole-allowed lowest excited state is expected to be larger than that of the ground state, since the excited state is coupled both to the ground state (by the same matrix element as the ground state is coupled to the lowest excited state) and to higher-lying dipole-allowed states. Note that a large value of the transition dipole moment can be related to a large exciton size (large electron-hole separation or diffuse character). One can also expect different trends for singlet and triplet states. For example, for the states of $\pi \rightarrow \pi^*$ character, the singlets should have larger polarizability than the triplets as the latter are not interacting with the ground state and are only coupled to the triplet manifold, which is less dense than the singlet manifold because the Pauli principle forbids certain electronic configurations (i.e., ionic) for the same-spin electrons. In contrast, singlet and triplet states of $n \rightarrow \pi^*$ character should have similar polarizabilities, since the singlets of this type have low oscillator strength and are coupled only to the excited state manifold.

A. Benchmark systems: Pyrimidine and s-tetrazine

Tables I and II compare the ground- and excited-state static polarizabilities for pyrimidine and s-tetrazine computed using our EOM-EE-CCSD implementations with the CCSD response-theory results from Ref. 20. Clearly, the analytic-derivative EOM-EE-CCSD implementation and CCSD response theory give identical results. In addition, the correctness of our analytic-derivative implementation is validated by the finite-field calculations.

For the CCSD ground state, the expectation-value approach yields the polarizabilities, which are within a few percent of the analytic-derivative (and finite-field) values.

TABLE I. Static polarizabilities (in a.u.) of the ground state ($\mu_z = 1.0$ a.u.) and the lowest singlet excited state ($E_{ex} = 4.59$ eV, $\mu_z = 0.3$ a.u.) of pyrimidine calculated with EOM-EE-CCSD/POL1.^a

	Ground state				1B_2 state			
	F.F. ^b	Ref. 20	E.V. ^c	Deriv. ^d	F.F. ^b	Ref. 20	E.V. ^c	Deriv. ^d
α_{xx}	67.8	67.8	70.0	67.8	111.8	111.8	103.0	111.8
α_{yy}	37.5	37.5	38.2	37.5	42.2	42.2	33.2	42.2
α_{zz}	70.2	70.2	72.5	70.2	71.4	71.4	51.2	71.4

^aDipole moments include orbital relaxation.

^bFinite-field approach.

^cExpectation-value approach.

^dAnalytic-derivative approach.

TABLE II. Static polarizabilities (in a.u.) of the ground state and the lowest singlet excited state ($E_{ex} = 2.39$ eV) of s-tetrazine calculated with EOM-EE-CCSD/POL1.

	Ground state				${}^1\text{B}_{1u}$ ex. state			
	F.F.	Ref. 20	E.V.	Deriv.	F.F.	Ref. 20	E.V.	Deriv.
α_{xx}	60.7	60.7	62.8	60.7	66.0	66.0 ^a	49.3	66.0
α_{yy}	56.0	56.0	58.0	56.0	80.1	80.1	71.7	80.1
α_{zz}	32.7	32.7	33.5	32.7	31.9	31.9	23.0	31.9

^aThe reported value of 61.5 for α_{zz} in Ref. 20 is a typo, as it is inconsistent with the reported anisotropy parameter, $\gamma = 41.1$. Using the values reported for γ , α_{xx} , and α_{yy} in Ref. 20, one obtains $\alpha_{zz} = 66.0$.

However, the differences become much larger (up to $\sim 30\%$) for the excited-state polarizabilities. Thus, the expectation-value approach, which is considerably cheaper in terms of computational cost and storage requirements, for calculating excited-state polarizabilities leads to noticeably different results compared to the analytic-derivative approach. In the rest of this paper, we focus on analytic-derivative polarizabilities only.

The ${}^1\text{B}_2$ state in pyrimidine and the ${}^1\text{B}_{1u}$ state in s-tetrazine are derived by the $n \rightarrow \pi^*$ transitions. Thus, the resulting exciton has a hole in the σ -system and an electron in the π -system. In both cases, the resulting state is more polarizable to in-plane perturbations, which can be rationalized by a higher mobility of the exciton in the molecular plane than in the π -system. The results for s-tetrazine are consistent with the findings in Refs. 15 and 20.

B. Uracil

Table III presents the excitation energies, dipole moments, and static polarizabilities of the ground state and the lowest singlet and triplet $n \rightarrow \pi^*$ and $\pi \rightarrow \pi^*$ states obtained with EOM-EE-CCSD and the aug-cc-pVDZ basis set. The discussion regarding the characters of these states and their EOM-CCSD description can be found in Ref. 66. Fig. 1 shows NTOs corresponding to these transitions.

The dipole moment and polarizability of the ground state of uracil computed with our implementation are similar to the CCSD linear response-theory results presented in Ref. 75.

TABLE III. Vertical excitation energies (in eV), dipole moments^a (in a.u.), and static polarizabilities (in a.u.) of the ground state and the singlet and triplet $n \rightarrow \pi^*$ and $\pi \rightarrow \pi^*$ states of uracil calculated with EOM-EE-CCSD/aug-cc-pVDZ.

Ground state	${}^1\text{A}''$ ($n \rightarrow \pi^*$)	${}^2\text{A}'$ ($\pi \rightarrow \pi^*$)	${}^1\text{A}'$ ($\pi \rightarrow \pi^*$)	${}^1\text{A}''$ ($n \rightarrow \pi^*$)
E_{ex}	...	5.22	5.58	3.87
μ_x	0.5	-0.4	1.3	0.3
μ_y	-1.6	-0.7	-1.8	-1.5
μ	1.7	0.9	2.2	1.5
α_{xx}	95.8	98.3	134.0	101.6
α_{yy}	74.6	88.3	102.7	85.2
α_{zz}	41.6	45.2	51.6	44.1
α_{iso}	70.7	77.2	96.1	77.0
				76.0

^aDipole moments include orbital relaxation.

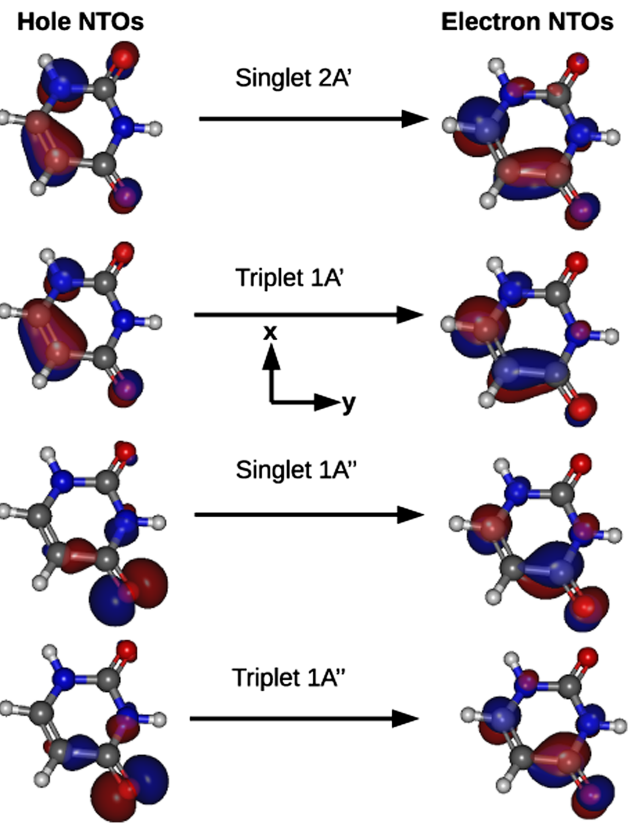


FIG. 1. Natural transition orbitals for the $n \rightarrow \pi^*$ and $\pi \rightarrow \pi^*$ states of uracil.

despite using a slightly different geometry and a smaller basis set (the aug-cc-pVTZ basis set was used in Ref. 75).

The lowest singlet excited state of uracil (${}^1\text{A}''$) corresponds to the $n \rightarrow \pi^*$ transition and has a vertical excitation energy of 5.22 eV. This state can be described as a transition from the in-plane lone pair orbital on the oxygen atom to the π^* -orbitals delocalized over all the heavy atoms (Fig. 1). As in the $n \rightarrow \pi^*$ states of pyrimidine and s-tetrazine, we observe increased polarizability for the in-plane perturbations, which we attribute to the larger mobility of the exciton in the molecular plane. The corresponding triplet state (${}^3\text{A}''$) shows the same behavior.

The excitation to the lowest singlet $\pi \rightarrow \pi^*$ (${}^1\text{A}'$) state (vertical excitation energy of 5.58 eV) results in a significant increase in both the dipole moment and polarizability. The change in the dipole moment is the largest along the x -direction. Both in-plane and out-of-plane components of polarizability increase, although the electronic structure is more polarizable for the in-plane perturbations with α_{xx} being the most affected and α_{zz} being the least affected. Relative to other states studied here, the larger change in polarizability for this transition is consistent with the non-zero transition moment. These results are in agreement with the findings in Ref. 75. As expected, we observe much smaller increase in polarizability for the triplet $\pi \rightarrow \pi^*$ state (because it is not dipole-coupled to the ground state). One can also rationalize larger polarizability of the singlet $\pi \rightarrow \pi^*$ state by noting that the change in dipole moment for the singlet $\pi \rightarrow \pi^*$ state is at an angle to the permanent dipole moment, while these quantities are more aligned for the triplet $\pi \rightarrow \pi^*$ state. Thus, the hole and

TABLE IV. Wave function analysis of the excited states of uracil. x -, y -, and z -components are given in parentheses.

	$1^1A''$ ($n \rightarrow \pi^*$)	$2^1A'$ ($\pi \rightarrow \pi^*$)	$1^3A'$ ($\pi \rightarrow \pi^*$)	$1^3A''$ ($n \rightarrow \pi^*$)
Transition $\mu_x^{0 \rightarrow f}$	0.0	1.1	0.0	0.0
Transition $\mu_x^{f \rightarrow 0}$	0.0	1.2	0.0	0.0
Transition $\mu_y^{0 \rightarrow f}$	0.0	-0.3	0.0	0.0
Transition $\mu_y^{f \rightarrow 0}$	0.0	-0.4	0.0	0.0
Participation ratio	1.01	1.15	1.08	1.02
$ \gamma^{0f} ^2$	0.81	0.81	0.85	0.83
Hole size (\AA)	1.39 (1.04, 0.84, 0.36)	1.95 (1.48, 1.04, 0.73)	1.79 (1.27, 0.99, 0.76)	1.36 (1.00, 0.85, 0.36)
Electron size (\AA)	1.84 (1.14, 1.23, 0.76)	2.01 (1.22, 1.34, 0.87)	1.78 (1.11, 1.15, 0.80)	1.81 (1.13, 1.20, 0.74)
RMS e^{-1} -hole	2.56	2.76	2.36	2.51
Separation (\AA)	(1.74, 1.69, 0.84)	(1.93, 1.62, 1.12)	(1.56, 1.40, 1.08)	(1.70, 1.65, 0.82)

electron sizes and the RMS electron-hole separation are larger, particularly along the x -axes for the singlet $\pi \rightarrow \pi^*$ state.

While the NTOs for the singlet and triplet states shown in Fig. 1 appear to be very similar, the wave function analysis of these states given in Table IV reveals quantitative differences between these states. The singlet states have larger hole- and electron-sizes as well as larger RMS electron-hole separation. Furthermore, these quantities are larger in the $\pi \rightarrow \pi^*$ states than in the $n \rightarrow \pi^*$ states.

C. Para-nitroaniline

The excitation energies, dipole moments, and static polarizabilities for the ground state and the lowest $\pi \rightarrow \pi^*$ singlet and triplet states of *p*-nitroaniline are given in Table V. Fig. 2 shows the respective NTOs. The wave function analysis is given in Table VI.

The $\pi \rightarrow \pi^*$ state in *p*-nitroaniline has significant charge-transfer character, as revealed by its large dipole moment. The increase in the dipole moment is considerably larger for the singlet excited state than for the triplet excited state due to the Pauli principle, which disfavors ionic configurations. This is consistent with the findings in Ref. 67. The isotropic static polarizability of both excited states is larger than that of the ground state. As in the previous examples, the exciton size is slightly larger in the singlet state than in the triplet (see Table VI). In contrast to uracil, the triplet excited state in

p-nitroaniline has slightly larger polarizability than the singlet excited state. This is possibly due to the highly ionic character of the singlet. For *p*-nitroaniline, the change in the dipole moment upon excitation is aligned with permanent dipole moment of the molecule. As a result, even though the hole and electron sizes and the RMS electron-hole separations for the singlet $\pi \rightarrow \pi^*$ state are larger, its more ionic electronic structure results in a smaller polarizability.

The polarizability of the singlet charge-transfer state has been studied previously by Jonsson *et al.*⁷⁶ using the cubic response theory for the CASSCF ground state and by Cammi *et al.*⁷⁷ using the linear response theory for the CASSCF excited states. While the use of slightly different geometry in our calculations compared to these previous studies is not expected to cause a significant change in the polarizability, the different basis sets used here could result in different

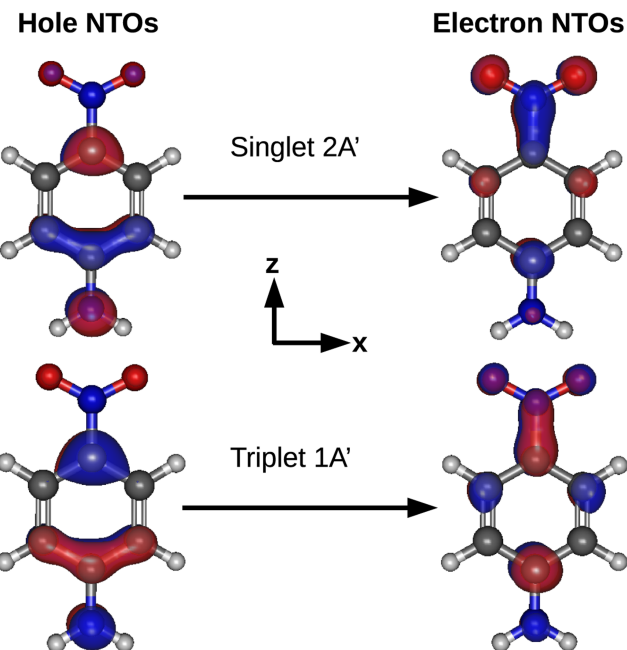


TABLE V. Excitation energies (in eV), dipole moments^a (in a.u.), and static polarizabilities (in a.u.) of the ground state and the $\pi \rightarrow \pi^*$ singlet and triplet states of *p*-nitroaniline calculated with EOM-EE-CCSD/aug-cc-pVDZ (the 6-31+G* values are given in parentheses).

	X^1A_1	2^1A_1	1^3A_1
E_{ex}	...	4.62 (4.66)	3.41 (3.43)
μ_z	-2.7 (-2.8)	-5.3 (-5.6)	-3.7 (-3.8)
α_{xx}	106.4 (101.0)	109.5 (104.9)	115.0 (110.1)
α_{yy}	56.9 (50.7)	83.5 (69.0)	61.7 (54.2)
α_{zz}	152.9 (143.5)	238.3 (222.1)	257.7 (253.2)
α_{iso}	105.4 (98.4)	144.1 (132.0)	144.8 (139.2)

^aDipole moments include orbital relaxation.

FIG. 2. Natural transition orbitals for the $\pi \rightarrow \pi^*$ states of *p*-nitroaniline.

TABLE VI. Wave function analysis of the excited states of *p*-nitroaniline with EOM-EE-CCSD/aug-cc-pVDZ. *x*-, *y*-, and *z*-components are given in parentheses.

	2^1A_1	1^3A_1
Transition $\mu_z^{0 \rightarrow f}$	-1.9	0.0
Transition $\mu_z^{f \rightarrow 0}$	-2.0	0.0
Participation ratio	1.13	1.21
$ \gamma^{0f} ^2$	0.77	0.83
Hole size (Å)	2.24 (0.82, 0.77, 1.93)	2.14 (0.85, 0.77, 1.80)
Electron size (Å)	2.53 (1.15, 0.83, 2.10)	2.37 (1.09, 0.79, 1.94)
RMS e ⁻¹ -hole separation (Å)	3.64 (1.40, 1.12, 3.17)	3.00 (1.29, 1.09, 2.48)

values for non-linear properties. This is, however, not seen in our calculations—the Pople and Dunning bases give similar results. While the individual polarizability components for the triplet do not increase much with the change of basis set from 6 to 31+G* to aug-cc-pVDZ, the increase for the singlet states is relatively larger. For both basis sets, the in-plane *xx*- and *zz*-components are larger for the triplet, but the perpendicular *yy*-component is larger for the singlet. Consistent with the previous studies, we see that the major contribution to the change in polarizability upon excitation comes from the in-plane components along the long axis (α_{zz}), while other components are affected less. We find that the change in the isotropic static polarizability upon excitation from the ground state of 38.7 a.u. with EOM-EE-CCSD/aug-cc-pVDZ is significantly larger than 6.1 a.u. calculated in Ref. 77. Interestingly, an even larger change of 44.7 a.u. in the isotropic static polarizability upon excitation from the ground state is reported from the double residue calculation of the cubic response function of the CASSCF ground state.

D. Diradicals: Methylenes and *para*-benzyne

Table VII presents the EOM-SF-CCSD/cc-pVTZ and EOM-EE-CCSD/cc-pVTZ vertical excitation energies, dipole moments, and static polarizabilities of the $M_s = 0$ triplet, open-shell singlet, and the two lowest closed-shell singlet states of methylene at four different geometries. The table also includes CCSD values for the singlet and high-spin triplet states. Clearly, the static polarizabilities of these states are similar and do not vary much across the four geometries. These states have relatively small values of the dipole moments and static polarizabilities.

Methylene has relatively weak diradical character (in the $\tilde{\alpha} 1^1\text{A}_1$ state), which can be well described by CCSD. The triplet and the open-shell singlet states are also described well by EOM-EE-CCSD with the respective energy gaps similar to the EOM-SF-CCSD values. However, the second closed-shell singlet state, $\tilde{c} 2^1\text{A}_1$, has significant doubly excited character relative to the low-spin reference employed in EOM-EE-CCSD and is, consequently, poorly described. The energy gap for this state relative to the triplet is also overestimated relative to the EOM-SF-CCSD values. The EOM-EE-CCSD static polarizabilities in Table VII (the numbers in parentheses) indicate that poor description of the $\tilde{c} 2^1\text{A}_1$ state significantly

TABLE VII. Excitation energies (in eV), dipole moments^a (in a.u.), and static polarizabilities (in a.u.) of the high-spin triplet reference, low-spin triplet, open-shell singlet, and two lowest closed-shell singlet states of methylene calculated with EOM-SF-CCSD/cc-pVTZ. The EOM-EE-CCSD values are given in the parentheses.

	$\tilde{X}^3\text{B}_2$ ($M_s = 1$)	$\tilde{X}^3\text{B}_2$	$\tilde{b}^1\text{B}_2$	$\tilde{\alpha} 1^1\text{A}_1$	$\tilde{c} 2^1\text{A}_1$
$\tilde{X}^3\text{B}_2$ geometry					
E_{ex}	-0.01	0.00 (0.00)	1.52 (1.53)	0.94 (1.01)	3.29 (4.95)
μ_z	-0.2	-0.2 (-0.2)	-0.3 (-0.3)	-0.6 (-0.6)	-0.1 (-0.1)
α_{xx}	13.3	13.3 (13.3)	13.5 (13.5)	15.0 (15.1)	12.5 (12.3)
α_{yy}	9.2	9.2 (9.1)	10.3 (12.0)	10.5 (10.9)	9.0 (6.1)
α_{zz}	9.8	9.8 (9.9)	10.2 (10.3)	12.6 (12.2)	8.6 (9.1)
α_{iso}	10.8	10.8 (10.8)	11.3 (11.9)	12.7 (12.8)	10.0 (9.1)
$\tilde{b}^1\text{B}_2$ geometry					
E_{ex}	-0.02	0.00 (0.00)	1.48 (1.49)	1.13 (1.23)	3.00 (4.60)
μ_z	-0.2	-0.2 (-0.2)	-0.3 (-0.3)	-0.5 (-0.5)	-0.1 (-0.1)
α_{xx}	13.3	13.3 (13.3)	13.5 (13.5)	14.6 (14.8)	12.7 (12.4)
α_{yy}	9.3	9.3 (9.5)	10.3 (16.5)	10.6 (10.2)	9.3 (1.1)
α_{zz}	9.7	9.7 (9.8)	10.1 (10.2)	12.7 (12.2)	8.1 (8.7)
α_{iso}	10.8	10.8 (10.8)	11.3 (13.4)	12.7 (12.4)	10.1 (7.4)
$\tilde{\alpha} 1^1\text{A}_1$ geometry					
E_{ex}	-0.01	0.00 (0.00)	1.74 (1.74)	-0.00 (0.02)	4.57 (6.38)
μ_z	-0.3	-0.3 (-0.3)	-0.4 (-0.4)	-0.7 (-0.7)	-0.2 (-0.1)
α_{xx}	13.1	13.1 (13.0)	13.3 (13.3)	15.2 (15.2)	11.9 (12.0)
α_{yy}	8.9	8.9 (8.9)	10.5 (10.5)	10.2 (10.3)	8.5 (8.2)
α_{zz}	11.4	11.4 (11.6)	11.8 (11.9)	13.1 (13.9)	11.0 (11.1)
α_{iso}	11.1	11.1 (11.1)	11.9 (11.9)	12.8 (13.1)	10.4 (10.4)
$\tilde{c} 2^1\text{A}_1$ geometry					
E_{ex}	-0.03	0.00 (0.00)	1.36 (1.38)	1.36 (1.68)	2.44 (3.76)
μ_z	-0.1	-0.1 (-0.1)	-0.1 (-0.1)	-0.1 (-0.2)	-0.1 (-0.0)
α_{xx}	12.7	12.7 (12.6)	12.7 (12.7)	12.7 (12.8)	12.8 (12.6)
α_{yy}	9.7	9.7 (9.8)	10.4 (10.9)	10.4 (7.5)	10.7 (13.5)
α_{zz}	9.7	9.7 (9.7)	10.3 (10.3)	11.0 (12.8)	10.2 (8.3)
α_{iso}	10.7	10.7 (10.7)	11.1 (11.3)	11.4 (11.1)	11.3 (11.5)

^aDipole moments include orbital relaxation.

affects the polarizability of not only the closed-shell singlet states but also the open-shell singlet state. For example, we note a large discrepancy between the EOM-EE-CCSD and EOM-SF-CCSD α_{yy} values (16.5 and 10.3 respectively) for the open-shell singlet state ($\tilde{b}^1\text{B}_2$) at the $\tilde{b}^1\text{B}_2$ geometry. The corresponding discrepancies in the α_{yy} -components of the closed-shell singlet states are also large along with the discrepancies in the excitation energies, which indicates a poor description of these states by EOM-EE-CCSD. Using the sum-over-states expression, we identify that the large discrepancy in the α_{yy} -component of the open-shell singlet state between the EOM-EE-CCSD and EOM-SF-CCSD calculations arises mainly due to the differences in the transition moments and energy gaps between the closed-shell singlet states ($\tilde{\alpha} 1^1\text{A}_1$ and $\tilde{c} 2^1\text{A}_1$) and the $\tilde{b}^1\text{B}_2$ state. Thus, reliable values of the polarizabilities depend on an accurate description of the entire energy spectrum and the respective transition moments.

Table VIII gives the vertical excitation energies, dipole moments, and the static polarizabilities for the low-spin $^3\text{B}_{2u}$

TABLE VIII. Excitation energies (in eV) and static polarizabilities (in a.u.) of the high-spin triplet reference; the $M_s = 0$ $^3\text{B}_{2u}$ state and the lowest $^1\text{A}_g$ singlet state of *p*-benzyne calculated with EOM-SF-CCSD/cc-pVTZ. The CCSD/EOM-EE-CCSD values are given in the parentheses.

	$^3\text{B}_{2u}$ ($M_s = 1$)	$^1\text{A}_g$	$^3\text{B}_{2u}$
$^1\text{A}_g$ geometry			
E_{ex}	0.20	—	0.22 (-0.55)
α_{xx}	76.7	76.2 (76.2)	76.7 (75.9)
α_{yy}	66.9	72.2 (78.5)	66.9 (61.8)
α_{zz}	32.9	32.4 (32.2)	32.9 (32.7)
α_{iso}	58.9	60.3 (62.3)	58.9 (56.8)
$^3\text{B}_{2u}$ geometry			
E_{ex}	0.11	—	0.14 (-0.74)
α_{xx}	77.2	76.5 (76.4)	77.1 (76.3)
α_{yy}	66.4	70.0 (75.7)	66.5 (61.0)
α_{zz}	33.0	32.5 (32.2)	33.0 (32.7)
α_{iso}	58.9	59.7 (61.5)	58.9 (56.7)

triplet state and the lowest $^1\text{A}_g$ singlet state of the $\sigma\sigma$ *p*-benzyne diradical calculated using EOM-SF-CCSD/cc-pVTZ. Large diradical character of the $^1\text{A}_g$ state makes its electronic structure similar to the triplet (i.e., low ionic character). As a result, the static polarizabilities for these two states are similar with the triplet state being slightly less polarizable along the short *y*-axis. CCSD is expected to describe $^1\text{A}_g$ poorly. The CCSD values for the $^1\text{A}_g$ state are different mainly in the α_{yy} -component. This is expected as the diradical centers lie on the *y*-axis. Similar differences between α_{yy} -components computed with CCSD and a multireference CCSD method have been reported in Ref. 78. We note that, unlike methylene, the polarizabilities of the low-spin triplet state computed with EOM-SF-CCSD and EOM-EE-CCSD are also different, mainly in the α_{yy} -component. Thus, strong diradical character of *p*-benzyne affects not only the singlet but also the triplet manifold. This is further confirmed by the fact that the CCSD polarizability of the high-spin triplet reference is similar to the EOM-SF-CCSD polarizability and not the EOM-EE-CCSD polarizability of the low-spin triplet state.

V. CONCLUSIONS

We presented the formalism and implementation for calculating the ground- and excited-state static polarizabilities within the EOM-EE-CCSD and EOM-SF-CCSD framework as analytic second derivatives with respect to the external electric-field perturbations. Our derivation is based on the asymmetric EOM-EE-CCSD formulation of the second-order static properties presented by Stanton and Gauss,³⁶ although the reformulation of the term involving the first-order response of the amplitude-response Lagrange multipliers results in a mixed symmetric-asymmetric formulation. Following others, we omit orbital relaxation in our formulation. The implementation is validated against previously reported CCSD response theory results²⁰ and finite-field calculations for the ground- and excited-states of pyrimidine and s-tetrazine. We also presented static polarizabilities for excited states of uracil and

p-nitroaniline. The EOM-EE-CCSD implementation has been extended to the EOM-SF-CCSD method, which enables calculations of the static polarizabilities of open-shell systems such as diradicals. Here, we report benchmark results for the methylene and *p*-benzyne diradicals. We find that even a weak diradical character (as in methylene) can lead to significant errors in the polarizabilities of the closed-shell and open-shell singlet states computed with EOM-EE-CCSD relative to the EOM-SF-CCSD method. In systems (such as *p*-benzyne) with strong diradical character, both singlet and triplet manifolds are affected.

Motivated by possible computational savings in terms of the response equations that need to be solved, we also discuss an alternative, simpler formalism and implementation for computing static polarizabilities as expectation values, wherein we employ the EOM-CCSD wave functions and energies in the exact sum-over-states expression of the polarizabilities. We found that while the expectation-value approach predicts similar-quality static polarizabilities for the CCSD reference relative to the analytic-derivative implementation, the results for the excited states may show large differences (up to ~30%).

SUPPLEMENTARY MATERIAL

See [supplementary material](#) for the programmable expressions of the CCSD/EOM-CCSD intermediates, DIIS setup, relevant Cartesian geometries, and a sample Q-Chem input.

ACKNOWLEDGMENTS

We thank Dr. Thomas Jagau and Professor Jürgen Gauss for helpful discussions and their comments on the manuscript. A.I.K. acknowledges the support by the U.S. National Science Foundation (Grant No. CHE-1566428).

- J. Olsen and P. Jørgensen, "Linear and non-linear response functions for an exact state and for MCSCF state," *J. Chem. Phys.* **82**, 3235 (1985).
- T. Helgaker, S. Coriani, P. Jørgensen, K. Kristensen, J. Olsen, and K. Ruud, "Recent advances in wave function-based methods of molecular-property calculations," *Chem. Rev.* **112**, 543 (2012).
- L. Pašteka, M. Melicherčík, P. Neogrády, and M. Urban, "CASPT2 and CCSD(T) calculations of dipole moments and polarizabilities of acetone in excited states," *Mol. Phys.* **110**, 2219 (2012).
- S. Klein, E. Kochanski, A. Strich, and A. J. Sadlej, "Electric properties of the water molecule in $^1\text{A}_1$, $^1\text{B}_1$, and $^3\text{B}_1$ electronic states: Refined CASSCF and CASPT2 calculations," *Theor. Chim. Acta* **94**, 75 (1996).
- P. B. Rozyczko, S. A. Perera, M. Nooijen, and R. J. Bartlett, "Correlated calculations of molecular dynamic polarizabilities," *J. Chem. Phys.* **107**, 6736 (1997).
- M. Mérawa and M. Réat, "*Ab initio* calculation of excited state dipole polarizability—application to the first $^1,^3\text{S}_{g,u}$ states of Li_2 ," *Eur. Phys. J. D* **17**, 329 (2001).
- G. Bublitz and S. Boxer, "Stark spectroscopy: Applications in chemistry, biology, and materials science," *Annu. Rev. Phys. Chem.* **48**, 213 (1997).
- R. Pauszek III, G. Kodali, and R. Stanley, "Excited state electronic structures of 5,10-methylenetetrahydrofolate and 5,10-methylenetetrahydrofolate determined by Stark spectroscopy," *J. Phys. Chem. A* **118**, 8320 (2014).
- V. Librando and A. Alparone, "Electronic polarizability as a predictor of biodegradation rates of dimethylnaphthalenes. An *ab initio* and density functional theory study," *J. Chem. Phys.* **41**, 1646 (2007).
- S. M. Smith, A. N. Markevitch, D. A. Romanov, X. Li, R. J. Levis, and H. B. Schlegel, "Static and dynamic polarizabilities of conjugated molecules and their cations," *J. Phys. Chem. A* **108**, 11063 (2004).
- K. Hald, F. Pawłowski, P. Jørgensen, and C. Hättig, "Calculation of frequency-dependent polarizabilities using the approximate coupled-cluster triples model CC3," *J. Chem. Phys.* **118**, 1292 (2003).

- ¹²M. Kállay and J. Gauss, "Calculation of frequency-dependent polarizabilities using general coupled-cluster models," *J. Mol. Struct.: THEOCHEM* **768**, 71 (2006).
- ¹³M. Urban and A. Sadlej, Molecular electric properties in electronic excited states: Multipole moments and polarizabilities of H₂O in the lowest B₁ and ³B₁ excited states, *Theor. Chim. Acta* **78**, 189 (1990).
- ¹⁴M. Medved, Š. Budzák, and T. Pluta, Electric properties of the low-lying excited states of benzonitrile: Geometry relaxation and solvent effects, *Theor. Chem. Acc.* **134**, 78 (2015).
- ¹⁵J. Stanton and J. Gauss, "The first excited singlet state of s-tetrazine: A theoretical analysis of some outstanding question," *J. Chem. Phys.* **104**, 9859 (1996).
- ¹⁶P. Norman, D. Jonsson, O. Vahtras, and H. Ågren, "Non-linear electric and magnetic properties obtained from cubic response functions in the random phase approximation," *Chem. Phys.* **203**, 23 (1996).
- ¹⁷D. Jonsson, P. Norman, and H. Ågren, "Cubic response functions in the multiconfiguration self-consistent field approximation," *J. Chem. Phys.* **105**, 6401 (1996).
- ¹⁸D. Jonsson, P. Norman, and H. Ågren, "Single determinant calculations of excited state polarizabilities," *Chem. Phys.* **224**, 201 (1997).
- ¹⁹B. Jansik, D. Jonsson, P. Salek, and H. Ågren, "Calculations of static and dynamic polarizabilities of excited states by means of density functional theory," *J. Chem. Phys.* **121**, 7595 (2004).
- ²⁰C. Hättig, O. Christiansen, S. Coriani, and P. Jørgensen, "Static and frequency-dependent polarizabilities of excited singlet states using coupled cluster response theory," *J. Chem. Phys.* **109**, 9237 (1998).
- ²¹N. Graf, D. Friese, N. Winter, and C. Hättig, "Excited state polarizabilities for CC2 using the resolution-of-the-identity approximation," *J. Chem. Phys.* **143**, 244108 (2015).
- ²²R. J. Bartlett, "Many-body perturbation theory and coupled cluster theory for electron correlation in molecules," *Annu. Rev. Phys. Chem.* **32**, 359 (1981).
- ²³R. J. Bartlett and J. F. Stanton, *Applications of Post-Hartree-Fock Methods: A Tutorial* (John Wiley & Sons, Inc., 1994), pp. 65–169.
- ²⁴R. J. Bartlett, "To multireference or not to multireference: That is the question?," *Int. J. Mol. Sci.* **3**, 579 (2002).
- ²⁵A. I. Krylov, "Equation-of-motion coupled-cluster methods for open-shell and electronically excited species: The hitchhiker's guide to Fock space," *Annu. Rev. Phys. Chem.* **59**, 433 (2008).
- ²⁶R. J. Bartlett, "The coupled-cluster revolution," *Mol. Phys.* **108**, 2905 (2010).
- ²⁷K. Sneskov and O. Christiansen, "Excited state coupled cluster methods," *Wiley Interdiscip. Rev.: Comput. Mol. Sci.* **2**, 566 (2012).
- ²⁸R. J. Bartlett, "Coupled-cluster theory and its equation-of-motion extensions," *Wiley Interdiscip. Rev.: Comput. Mol. Sci.* **2**, 126 (2012).
- ²⁹J. F. Stanton and R. J. Bartlett, "The equation of motion coupled-cluster method. A systematic biorthogonal approach to molecular excitation energies, transition probabilities, and excited state properties," *J. Chem. Phys.* **98**, 7029 (1993).
- ³⁰L. V. Slipchenko, "Solvation of the excited states of chromophores in polarizable environment: Orbital relaxation versus polarization," *J. Phys. Chem. A* **114**, 8824 (2010).
- ³¹K. Nanda and A. I. Krylov, "Two-photon absorption cross sections within equation-of-motion coupled-cluster formalism using resolution-of-the-identity and Cholesky decomposition representations: Theory, implementation, and benchmarks," *J. Chem. Phys.* **142**, 064118 (2015).
- ³²K. Klein and J. Gauss, "Perturbative calculation of spin-orbit splittings using the equation-of-motion ionization-potential coupled-cluster ansatz," *J. Chem. Phys.* **129**, 194106 (2008).
- ³³E. Epifanovsky, K. Klein, S. Stopkowicz, J. Gauss, and A. I. Krylov, "Spin-orbit couplings within the equation-of-motion coupled-cluster framework: Theory, implementation, and benchmark calculations," *J. Chem. Phys.* **143**, 064102 (2015).
- ³⁴A. I. Krylov, "The quantum chemistry of open-shell species," in *Reviews in Computational Chemistry*, edited by A. L. Parrill and K. B. Lipkowitz (John Wiley & Sons, 2017), Chap. 4.
- ³⁵J. F. Stanton, "Many-body methods for excited state potential energy surfaces. I. General theory of energy gradients for the equation-of-motion coupled-cluster method," *J. Chem. Phys.* **99**, 8840 (1993).
- ³⁶J. F. Stanton and J. Gauss, "Many-body methods for excited state potential energy surfaces. II. Analytic second derivatives for excited state energies in the equation-of-motion coupled-cluster method," *J. Chem. Phys.* **103**, 8931 (1995).
- ³⁷J. F. Stanton and J. Gauss, "Analytic energy gradients for the equation-of-motion coupled-cluster method: Implementation and application to the HCN/HNC system," *J. Chem. Phys.* **100**, 4695 (1994).
- ³⁸S. V. Levchenko, T. Wang, and A. I. Krylov, "Analytic gradients for the spin-conserving and spin-flipping equation-of-motion coupled-cluster models with single and double substitutions," *J. Chem. Phys.* **122**, 224106 (2005).
- ³⁹K. Klein, *Analytische Ableitungen der Energie für den "Equation-of-Motion-Coupled-Cluster"-Ansatz zur Berechnung von Ionisationspotentialen* (Johannes-Gutenberg Universität, Mainz, 2014).
- ⁴⁰T. Helgaker, P. Jørgensen, and J. Olsen, *Molecular Electronic Structure Theory* (Wiley & Sons, 2000).
- ⁴¹P. G. Szalay, "Analytic energy derivatives for coupled-cluster methods describing excited states: General formulas and comparison of computational costs," *Int. J. Quantum Chem.* **55**, 151 (1995).
- ⁴²S. R. Gwaltney and R. J. Bartlett, "Gradients for the partitioned equation-of-motion coupled-cluster method," *J. Chem. Phys.* **110**, 62 (1999).
- ⁴³F. Furche and R. Ahlrichs, "Adiabatic time-dependent density functional methods for excited state properties," *J. Chem. Phys.* **117**, 7433 (2002).
- ⁴⁴P. Celani and H.-J. Werner, "Analytical energy gradients for internally contracted second-order multireference perturbation theory," *J. Chem. Phys.* **119**, 5044 (2003).
- ⁴⁵P. Pulay, "Second and third derivatives of variational energy expressions: Application to multiconfigurational selfconsistent field wave functions," *J. Chem. Phys.* **78**, 5043 (1983).
- ⁴⁶P. Jørgensen, P. Swanstrøm, D. Yeager, and J. Olsen, "Multiconfigurational Hartree-Fock response functions," *Int. J. Quantum Chem.* **23**, 959 (1983).
- ⁴⁷P. Jørgensen and T. Helgaker, "Möller-plesset energy derivatives," *J. Chem. Phys.* **89**, 1560 (1988).
- ⁴⁸T. Helgaker and P. Jørgensen, "Configuration-interaction energy derivatives in a fully variational formulation," *Theor. Chim. Acta* **75**, 111 (1989).
- ⁴⁹H. Koch, R. Kobayashi, A. S. de Merás, and P. Jørgensen, "Calculation of size-extensive transition moments from coupled cluster singles and doubles linear response function," *J. Chem. Phys.* **100**, 4393 (1994).
- ⁵⁰P. Rozyczko and R. J. Bartlett, "Frequency dependent equation-of-motion coupled cluster hyperpolarizabilities: Resolution of the discrepancy between theory and experiment for HF?," *J. Chem. Phys.* **107**, 10823 (1997).
- ⁵¹F. Pawłowski, J. Olsen, and P. Jørgensen, "Molecular response properties from a Hermitian eigenvalue equation for a time-periodic Hamiltonian," *J. Chem. Phys.* **142**, 114109 (2015).
- ⁵²S. Coriani, F. Pawłowski, J. Olsen, and P. Jørgensen, "Molecular response properties in equation of motion coupled cluster theory: A time-dependent perspective," *J. Chem. Phys.* **144**, 02410 (2016).
- ⁵³K. Kamada, K. Ohta, T. Kubo, A. Shimizu, Y. Morita, K. Nakasui, R. Kishi, S. Ohta, S. Furukawa, H. Takahashi, and M. Nakano, "Strong two-photon absorption of singlet diradical hydrocarbons," *Angew. Chem. Int. Ed.* **46**, 3544 (2007).
- ⁵⁴S. Thomas and K. S. Kim, "Linear and nonlinear optical properties of indeno[2,1-b]fluorene and its structural isomers," *Phys. Chem. Chem. Phys.* **16**, 24592 (2014).
- ⁵⁵M. Nakano and B. Champagne, "Diradical character dependence of third-harmonic generation spectra in open-shell singlet systems," *Theor. Chim. Acta* **134**, 23 (2015).
- ⁵⁶K. Kamada, S. Fuku-en, S. Minamide, K. Ohta, R. Kishi, M. Nakano, H. Matsuzaki, H. Okamoto, H. Higashikawa, K. Inoue, S. Kojima, and Y. Yamamoto, "Impact of diradical character on two-photon absorption: Bis(acridine) dimers synthesized from an allenic precursor," *J. Am. Chem. Soc.* **135**, 232 (2013).
- ⁵⁷Z. Zeng, S. Lee, M. Son, K. Fukuda, P. M. Burrezo, X. Zhu, Q. Qi, R.-W. Li, J. T. López, N. J. Ding, J. Casado, M. Nakano, D. Kim, and J. Wu, "Push-pull type oligo(n-annulated perylene)quinoxidimethanes: Chain length and solvent-dependent ground states and physical properties," *J. Am. Chem. Soc.* **137**, 8572 (2015).
- ⁵⁸The reference determines the separation of orbital space into the occupied and virtual subspaces. Here we use indexes i, j, k, \dots and a, b, c, \dots to denote the orbitals from the two subspaces. To denote orbitals that can be either occupied or virtual, letters p, q, r, s, \dots will be used.
- ⁵⁹S. V. Levchenko and A. I. Krylov, "Equation-of-motion spin-flip coupled-cluster model with single and double substitutions: Theory and application to cyclobutadiene," *J. Chem. Phys.* **120**, 175 (2004).
- ⁶⁰Y. Shao, Z. Gan, E. Epifanovsky, A. T. B. Gilbert, M. Wormit, J. Kussmann, A. W. Lange, A. Behn, J. Deng, X. Feng, D. Ghosh, M. Goldey, P. R. Horn,

- L. D. Jacobson, I. Kaliman, R. Z. Khaliullin, T. Kus, A. Landau, J. Liu, E. I. Proynov, Y. M. Rhee, R. M. Richard, M. A. Rohrdanz, R. P. Steele, E. J. Sundstrom, H. L. Woodcock III, P. M. Zimmerman, D. Zuev, B. Albrecht, E. Alguires, B. Austin, G. J. O. Beran, Y. A. Bernard, E. Berquist, K. Brandhorst, K. B. Bravaya, S. T. Brown, D. Casanova, C.-M. Chang, Y. Chen, S. H. Chien, K. D. Closser, D. L. Crittenden, M. Diedenhofen, R. A. DiStasio, Jr., H. Do, A. D. Dutoi, R. G. Edgar, S. Fatehi, L. Fusti-Molnar, A. Ghysels, A. Golubeva-Zadorozhnaya, J. Gomes, M. W. D. Hanson-Heine, P. H. P. Harbach, A. W. Hauser, E. G. Hohenstein, Z. C. Holden, T.-C. Jagau, H. Ji, B. Kaduk, K. Khistyayev, J. Kim, J. Kim, R. A. King, P. Klunzinger, D. Kosenkov, T. Kowalczyk, C. M. Krauter, K. U. Laog, A. Laurent, K. V. Lawler, S. V. Levchenko, C. Y. Lin, F. Liu, E. Livshits, R. C. Lochan, A. Luenser, P. Manohar, S. F. Manzer, S.-P. Mao, N. Mardirossian, A. V. Marenich, S. A. Maurer, N. J. Mayhall, C. M. Oana, R. Olivares-Amaya, D. P. O'Neill, J. A. Parkhill, T. M. Perrine, R. Peverati, P. A. Pieniazek, A. Prociuk, D. R. Rehn, E. Rosta, N. J. Russ, N. Sergueev, S. M. Sharada, S. Sharmaa, D. W. Small, A. Sodt, T. Stein, D. Stuck, Y.-C. Su, A. J. W. Thom, T. Tsuchimochi, L. Vogt, O. Vydrov, T. Wang, M. A. Watson, J. Wenzel, A. White, C. F. Williams, V. Vanovschi, S. Yeganeh, S. R. Yost, Z.-Q. You, I. Y. Zhang, X. Zhang, Y. Zhou, B. R. Brooks, G. K. L. Chan, D. M. Chipman, C. J. Cramer, W. A. Goddard III, M. S. Gordon, W. J. Hehre, A. Klamt, H. F. Schaefer III, M. W. Schmidt, C. D. Sherrill, D. G. Truhlar, A. Warshel, X. Xu, A. Aspuru-Guzik, R. Baer, A. T. Bell, N. A. Besley, J.-D. Chai, A. Dreuw, B. D. Dunietz, T. R. Furlani, S. R. Gwaltney, C.-P. Hsu, Y. Jung, J. Kong, D. S. Lambrecht, W. Z. Liang, C. Ochsenfeld, V. A. Rassolov, L. V. Slipchenko, J. E. Subotnik, T. Van Voorhis, J. M. Herbert, A. I. Krylov, P. M. Gill, and M. Head-Gordon, "Advances in molecular quantum chemistry contained in the Q-Chem 4 program package," *Mol. Phys.* **113**, 184 (2015).
- ⁶¹A. I. Krylov and P. M. W. Gill, "Q-Chem: An engine for innovation," *Wiley Interdiscip. Rev.: Comput. Mol. Sci.* **3**, 317 (2013).
- ⁶²E. Epifanovsky, M. Wormit, T. Kuš, A. Landau, D. Zuev, K. Khistyayev, P. Manohar, I. Kaliman, A. Dreuw, and A. I. Krylov, "New implementation of high-level correlated methods using a general block-tensor library for high-performance electronic structure calculations," *J. Comput. Chem.* **34**, 2293 (2013).
- ⁶³R. S. Mulliken, "Report on notation for the spectra of polyatomic molecules," *J. Chem. Phys.* **23**, 1997 (1955).
- ⁶⁴See <http://openshell.usc.edu/resources/howto/symmetry> for depending on molecular orientation, symmetry labels corresponding to the same orbital or vibrational mode may be different. Q-Chem's standard molecular orientation is different from that of Mulliken.⁶³ For example, Q-Chem places water molecule in *xz*-plane instead of *yz*. Consequently, for C_{2v} symmetry, b_1 and b_2 labels are flipped.
- ⁶⁵A. Sadlej, "Medium-size polarized basis sets for high-level correlated calculations of molecular electric properties," *Collect. Czech. Chem. Commun.* **53**, 1995 (1988).
- ⁶⁶E. Epifanovsky, K. Kowalski, P.-D. Fan, M. Valiev, S. Matsika, and A. I. Krylov, "On the electronically excited states of uracil," *J. Phys. Chem. A* **112**, 9983 (2008).
- ⁶⁷D. Kosenkov and L. V. Slipchenko, "Solvent effects on the electronic transitions of p-nitroaniline: A QM/EFP study," *J. Phys. Chem. A* **115**, 392 (2011).
- ⁶⁸F. Plasser, M. Wormit, and A. Dreuw, "New tools for the systematic analysis and visualization of electronic excitations. I. Formalism," *J. Chem. Phys.* **141**, 024106 (2014).
- ⁶⁹F. Plasser, S. A. Bäppler, M. Wormit, and A. Dreuw, "New tools for the systematic analysis and visualization of electronic excitations. II. Applications," *J. Chem. Phys.* **141**, 024107 (2014).
- ⁷⁰A. Allouche, "Gabedit-a graphical user interface for computational chemistry softwares," *J. Comput. Chem.* **32**, 174 (2011).
- ⁷¹L. V. Slipchenko and A. I. Krylov, "Singlet-triplet gaps in diradicals by the spin-flip approach: A benchmark study," *J. Chem. Phys.* **117**, 4694 (2002).
- ⁷²P. U. Manohar and A. I. Krylov, "A non-iterative perturbative triples correction for the spin-flipping and spin-conserving equation-of-motion coupled-cluster methods with single and double substitutions," *J. Chem. Phys.* **129**, 194105 (2008).
- ⁷³Y. A. Bernard, Y. Shao, and A. I. Krylov, "General formulation of spin-flip time-dependent density functional theory using non-collinear kernels: Theory, implementation, and benchmarks," *J. Chem. Phys.* **136**, 204103 (2012).
- ⁷⁴C. D. Sherrill, M. L. Leininger, T. J. Van Huis, and H. F. Schaefer III, "Structures and vibrational frequencies in the full configuration interaction limit: Predictions for four electronic states of methylene using triple-zeta plus double polarization (TZ2P) basis," *J. Chem. Phys.* **108**, 1040 (1998).
- ⁷⁵T. Pluta, M. Kolaski, M. Medved, and S. Budzák, "Dipole moment and polarizability of the low-lying excited states of uracil," *Chem. Phys. Lett.* **546**, 24 (2012).
- ⁷⁶D. Jonsson, P. Norman, H. Ågren, Y. Luo, K. Sylvester-Hvid, and K. Mikkelsen, "Excited state polarizabilities in solution obtained by cubic response theory: Calculations on para-, ortho-, and meta-nitroaniline," *J. Chem. Phys.* **109**, 6351 (1998).
- ⁷⁷R. Cammi, L. Frediani, B. Mennucci, and K. Ruud, "Multiconfigurational self-consistent field linear response for the polarizable continuum model: Theory and application to ground and excited-state polarizabilities of para-nitroaniline in solution," *J. Chem. Phys.* **119**, 5818 (2003).
- ⁷⁸T. Jagau and J. Gauss, "Linear-response theory for Mukherjee's multireference coupled-cluster method: Static and dynamic polarizabilities," *J. Chem. Phys.* **137**, 044115 (2012).